

Synthesis and Study of Mechanical and Electrical Properties of Poly S.I.S/PPY- V_2O_5 Polymeric Nano-Composites



Rabia Batool

Reg. # 172927

A thesis submitted in partial fulfillment of the requirements
for the degree of **Master of Science**

in

Chemistry


Supervised by: Dr. Mudassir Iqbal

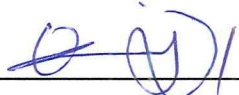
Department of chemistry
School of Natural Sciences
National University of Sciences and Technology
H-12, Islamabad, Pakistan
2016-18

National University of Sciences & Technology**MS THESIS WORK**

We hereby recommend that the dissertation prepared under our supervision by: RABIA BATOOL, Regn No. 00000117013 Titled: Synthesis And Studies Of Mechanical And Electrical Properties Of Poly S.I.S/Ppy-V205 Polymeric Nano-Composites be accepted in partial fulfillment of the requirements for the award of **MS** degree.

Examination Committee Members

1. Name: DR. TAYYABA NOOR Signature: 

2. Name: DR. QURRAT UL AIN JAVED Signature: 

External Examiner: DR. TAHIR MEHMOOD Signature: 


Supervisor's Name: DR. MUDASSIR IQBAL Signature: 


Head of Department

07/01/19
Date

COUNTERSIGNED

Date: 07/01/19


Dean/Principal

THESIS ACCEPTANCE CERTIFICATE

Certified that final copy of MS thesis written by **Ms. Rabia Batool**, (Registration No. **00000117013**), of **School of Natural Sciences** has been vetted by undersigned, found complete in all respects as per NUST statutes/regulations, is free of plagiarism, errors, and mistakes and is accepted as partial fulfillment for award of MS/M.Phil degree. It is further certified that necessary amendments as pointed out by GEC members and external examiner of the scholar have also been incorporated in the said thesis.

Signature:  _____

Name of Supervisor: Dr. Mudassir Iqbal

Date: 07/01/19

Signature (HoD):  _____

Date: 07/01/19

Signature (Dean/Principal):  _____

Date: 07/01/19

Dedication

*Dedicated to my beloved Grand-Parents and my Parents
Mr. /Mrs. Zafar Abbas.*

Acknowledgements

*I am grateful to the Creator **Almighty Allah** to have guided me throughout this work and for every new thought which He setup in my mind to enhance it.*

*I am generously thankful to my **Parents** who raised me when I was not even capable of strolling and kept supporting me.*

*My sincerely thanks goes to my thesis supervisor **Dr. Mudassir Iqbal** for all his inspiration, motivation and guidance throughout my research work. Without his support, I might be not able to achieve my goal.*

*I am also thankful to my GEC members **Dr. Qurat ul ain** and **Dr. Tayyaba Noor** for their constructive criticism and instructions for improvement. I also want to thank to HoD chemistry, **Dr. Muhammad Arfan** for his moral support and continuous efforts throughout the academics and School of Natural Sciences (SNS) for financial support during MS study. I am thankful to Principal SNS **Prof. Dr. Habib Nasir** for listening to our research related problems and accommodating us with the best possible solutions. I also acknowledge **NUST (National University of Science and Technology)** and all its departments (**SMME, IESE and CASEN**) for the facilities and technical support.*

*I would like to extend my gratitude to lab technician **Mr. Ishrat** for his Assistance during my lab work.*

*A special thanks to my lab fellows and friends **Bushra Rahat, Faiza Lughmani, Shoaib-ur-rehman, Farrea Batoool, M. Tayyab Ishaq, Sania Qurat ul ain, Sundas Tehreem, Muhammad Ishaq(QAU)** for their help, courage, motivation and boosting comments during my study.*

*Lastly I would like to thank my siblings **Yasir Abbas, Qaisar Abbas, Safder Abbas and Aliya Batoool** for their continuous support and affection.*

RABIA BATOOL

Abstract:

The increase in mechanical strength of polymer is comparatively higher at nano scale than large scale reinforcement. In current research scientist have work hard to develop polymer reinforced by nano particles and have obtained good results. The increase in mechanical strength can be improved by maintaining the fine dispersion of nano-particles within the polymer matrix and by the modification of the surface of nano-particles that act as reinforcement phase. Conducting polymers i-e polypyrrole, polythiophene, polyaniline or 3-methoxy derivative show electric conductivity due to the presence of p-system. These polymers have poly-conjugation showing electronic behavior of metals retaining their strength and processibility. Their conductivity can be increased by adding small amount of impurities i-e dopant into original polymer matrix. This can be done by p or n-type doping of polymer. Polypyrrole being conductive is stable to heat and environmental conditions and its chemical as well as electric oxidation is facile. The stability and electronic properties of polypyrrole can be increased by making blends with thermoplastic polymers. Polymers with conducting properties i-e polythiophene, polyaniline and polypyrrole are mixed with some thermoplastic polymer like polystyrene, polyvinylchloride help in enhancing stability. Nano-particles because of their high surface area show extensive interaction with any system they are dispersed in. Polymer nano composites are prepared by the incorporation of nano particles in to the polymer matrix here nano particles act as reinforcing phase. Nano particles increase the mechanical properties i-e Tensile strength, compressive strength, hardness, toughness, elasticity, plasticity etc. Polymer nano composites by enhancement of mechanical strength seek interest in variety of automotive and industrial applications i-e covers of various portable devices, vacuum cleaner blades and EMI shielding etc.

Contents:

Chapter 1:.....	12
Introduction	12
1.1 Polymer	12
1.2 Conducting polymer.....	13
1.3 Electrical Conductivity in polymers:.....	15
1.3.1 Band theory:.....	15
1.3.2Doping in insulating polymers:	17
1.3.3 Bolaron and bi-polaron model:.....	18
1.4 Polypyrrole as conducting polymer	19
1.5 Synthesis of Polypyrrole:.....	21
1.5.1 Chemical polymerization of Polypyrrole:.....	21
1.6 Polymer blends:	23
1.6.1 Classification Of polymeric blends:	23
1.6.2 Methods of blending:.....	24
1.7 Copolymer:.....	24
1.7.1 Structure and properties of SIS copolymer:.....	26
1.8 Nanomaterial:	27
1.8.1 Different approaches for Synthesis of nano-particles:	28
1.9 Nano-composites:	29
1.9.1 Classification of nano-composites:	29
1.9.2 Applications of polymeric nano-composites:	30
1.9.3 Nano-composites fabrication method:.....	31
Chapter 2.....	32
Literature review:.....	32
2.1 Green synthesis of nano-particles:	32
2.2 Polypyrrole blends:	33
2.3 Polymeric nano-composites:.....	34
Motivation:.....	39
Chapter 3:.....	39
Experimental.....	39
3.1 Materials:	39
3.2 Green synthesis of nano-particles:	39

3.2.1 Composition of green tea (<i>Camellia Sinensis</i>):	40
3.2.2 Preparation of green tea extract:	41
3.2.3 Preparation of vanadium penta-oxide nano-particles:.....	41
3.3 Synthesis of polypyrrole:.....	42
3.4 Synthesis of PPy/SIS blends:	43
3.5 Polymeric nano-composite formation V ₂ O ₅ /PPy-SIS blends:.....	43
3.6 Characterization techniques:	44
3.6.1 X-ray Diffractometer:.....	44
3.6.2 Fourier transform infrared spectroscopy:	47
3.6.3 Scanning electron microscopy coupled with EDX.....	49
3.6.4 Mechanical testing:	52
3.6.5 Two point probe conductivity measurement:	55
Chapter 4.....	57
Results and discussion	57
4.1 Synthesis and characterization of V ₂ O ₅ nano-particles:	57
4.1.1 Synthesis of V ₂ O ₅ nano-particles:	57
4.1.2 X-ray diffraction analysis of V ₂ O ₅ nano-particles	58
4.1.3 FT-IR analysis for V ₂ O ₅ nano-particles:	58
4.1.4 Energy dispersive X-ray spectroscopy:.....	59
4.2 Formation and characterization of polypyrrole:.....	60
4.2.1 Synthesis of polypyrrole:	60
4.2.2 X-ray Diffractometer:	61
4.2.3 FT-IR analysis of polypyrrole:	61
4.3 Formation and characterization of Poly SIS/PPY blends:.....	62
4.3.1 Synthesis of Poly SIS/PPY blends:	62
4.4 Formation and characterization of Poly SIS/PPY-V ₂ O ₅ polymeric nano-composites:.....	64
4.4.1 Formation of polymeric nano-composites:	64
4.4.2 Mechanical testing of Poly SIS/PPY-V ₂ O ₅ Composites:	64
4.5 Conclusions:	68
References:	70

List of Abbreviations:

CB	Conducting band
CPs	Conducting polymers
EC	Epicatechin
ECG	Epicatechin-3-gallate
EGC	Epigallocatechin
EGCG	Epigallocatechin-3-galla
eV	Electron Volt
FTIR	Fourier transform infrared spectroscopy
HOMO	Highest occupied molecular orbital
LUMO	Lowest unoccupied molecular orbital
HMPSAS	Hot melt pressure sensitive adhesives
MgO	Magnesium oxide
1D	One dimensional
PPO	Poly (phenylene oxide)
PP	Polypropylene
PA	Polyamide
PPy	Polypyrrole
PVC	Polyvinyl chloride
PANI	Polyaniline
SBS	Poly (styrene-butadiene-styrene)
SIS	Poly (styrene-isoprene-styrene)
ClO ₄ ⁻	Perchlorate anion
K ₂ S ₂ O ₈	Potassium peroxodisulfate
SDS	Sodium dodecyl sulfate
SEM	Scanning electron microscopy
T _m	True melt temperature

TEM	Transmission electron microscopy
TGA	Thermal gravimetric analysis
VB	Valence band
ASTM	American Society for Testing and Materials
V ₂ O ₅	Vanadium penta oxide
XRD	X-ray diffractometer
SEM	scanning electron microscopy
PS	Polystyrene
DNA	Deoxyribonucleic acid
RNA	ribonucleic acid
THF	Tetrahydrofuran
DMSO	Dimethyl sulfoxide
CNT	Carbon nano-tubes
MWCTs	Multi-walled carbon nano-tubes

Table of figures:

Figure 1. 1 Conducting polymers	13
Figure 1. 2 Noble prize winner for conducting polymers.....	14
Figure 1.4 Conduction in conducting polymers	17
Figure 1.5 Doped Polypyrrole	18
Figure 1.6 Band theory.....	19
Figure 1. 8 Polymerization of polypyrrole.....	20
Figure 1. 9 Energy level diagram of (a) Neutral PPy (b) Polaron (c) Bi-polaron.....	21
Figure 1. 10 Scheme of cation radical polymerization	22
Figure 1. 11 Polymerization of Polypyrrole.....	23
Figure 1. 12 Types of copolymer	25
Figure 1.13 SIS block copolymer	26
Figure 1.14 Structure of SIS copolymer	27
Figure 1. 15 top-down and bottom-up approach for synthesis of nano-particles	28
Figure 3. 1 Phenolic catechins in green tea leaves	40
Figure 3. 2 Synthesis of green tea extract and V ₂ O ₅ nano-particles.....	41
Figure 3. 3 Synthesis scheme of polypyrrole	42
Figure 3. 4 X-rays diffraction from crystal plane.....	45
Figure 3.5 Simple X-ray diffractometer.....	46
Figure 3. 6: <i>Different types of stretching and bending vibrations</i>	48
Figure 3.7 Fourier transform infrared spectroscopy.....	49
Figure 3. 8: Schematic of scanning electron microscopy	50
Figure 3. 9: Different signals generated by specimen-electron beam interaction.....	51
Figure 3. 10 Schematic representation of tensile testing machine	53
Figure 3. 11 Young's modulus determination.....	54
Figure 3. 12: Reduction in area under curve with increase in strength.....	55
Figure 3. 13: Two point probe conductivity measurement	56
Figure 4.1 XRD of V ₂ O ₅ nano-particles.....	58
Figure 4. 2: FT-IR of V ₂ O ₅ nano-particles and Green tea extract.....	59
Figure 4.3 : EDS for V ₂ O ₅ nano-particles.....	60
Figure 4. 4: XRD pattern of polypyrrole.....	61
Figure 4. 6: FT-IR of Poly SIS/PPY blend and SIS polymer.....	63
Figure 4. 7: FT-IR comparison of poly SIS/PPY and pure SIS	64
Figure 4. 8 Stress vs. % strain curve for (a) 0 %, (b) 6%, (c) 4%, (d) 2% blend	65
Figure 4. 9 Stress vs % strain curve for composites (a) 6% V ₂ O ₅ composite (b) 4% V ₂ O ₅ composite (c) 2% V ₂ O ₅ composite	67

List of tables:

Table 1. 1 Classification of polymers on the basis of different properties	12
Table 3. 1 PPy/SIS blends with different weight percent	43
Table 3. 2 V ₂ O ₅ /PPy-SIS nano-composites with different wt. %	44
Table 3. 3: Indexing of XRD data	46
Table 3. 4 Tensile test specimen dimensions.....	54
Table 4. 1 Young's modulus for 0%, 2%, 4%, 6% Poly SIS/PPY blends	66
Table 4. 2 Young's modulus for 2%, 4%, 6% poly SIS/PPY-V ₂ O ₅ Composites.....	68

Chapter 1:

Introduction

1.1 Polymer

The polymer is composed of two words –poly means "many" and –mers mean "units" or "segments". These units or segments link together via chemical bonding forming long chains known as polymers whereas these units or segments are called monomers. The chemical reaction resulting in the formation of polymer is known as polymerization [1]. Polymer exists in natural or synthetic form. Natural polymer existed since mankind's birth i.e. DNA, RNA, Proteins and polysaccharides. In 18th century scientists worked on modification of natural rubber by blending it with certain additives. Bakelite was the first synthetic polymer produced in 1909. Polymers can be categorized into different ways according to their physical, chemical, mechanical and thermal properties that can be summarized as given in table 1.1

Basis for classification	Type of polymer
Origin	Semi-synthetic, Synthetic, Natural polymer
Mode of synthesis	Condensation or Addition polymerization
Thermal properties	Thermosetting or Thermoplastic polymer
Structure	Cross-linked , Branched or linear
Crystallinity	Crystalline , Non-crystalline or Semi-crystalline
Tacticity	Atactic , Isotactic or Syndiotactic
Polarity	Non-polar or Polar
Chain	Homo or Hetero-chain
Physical properties	Fiber , Rubber or Plastic

Table 1. 1 Classification of polymers on the basis of different properties

Polymers are of two types on the basis of the response to applied thermal changes i.e. thermosetting and thermoplastic polymers. Thermoplastic polymers i.e. Nylon, PVC or Sealing wax can be plasticized or softened on thermal treatment in controlled conditions showing no change in

properties. Whereas thermosetting polymer i.e epoxy resins, urea or diene rubbers on thermal treatment convert into infusible solid mass [2, 3].

1.2 Conducting polymer

Conducting polymer contain aromatic ring as polymer backbone that results in delocalization of electrons promoting electrical conductivity by adding small quantity of dopant (K.G et al, 1998) [4].The conductivity in polymers can be increased up to metallic level using dopant via electrochemical or chemical p -type doping or n-type doping also known as oxidation or reduction. Conducting polymers (CPs) are very interesting materials as they show enhanced electrical conductivities while restoring thermal and mechanical properties. Conducting polymers have taken scientist's interest since being discovered in 1977[5].CPs exhibits distinctive electronic properties like optical transmission, high electron affinities, low ionization potential and low energies . The electrical conductivities of polymer are influenced by mobility, density and direction of charge carriers, presence of doping material and temperature change. CPs can be used in wet or dry state depending on electrical conductivity, porosity in their structure or polymer's processibility in micro structuring mechanism [6]. Examples for conducting polymers are polyaniline, polypyrrole, polythiophene and polyacetylene etc shown below:

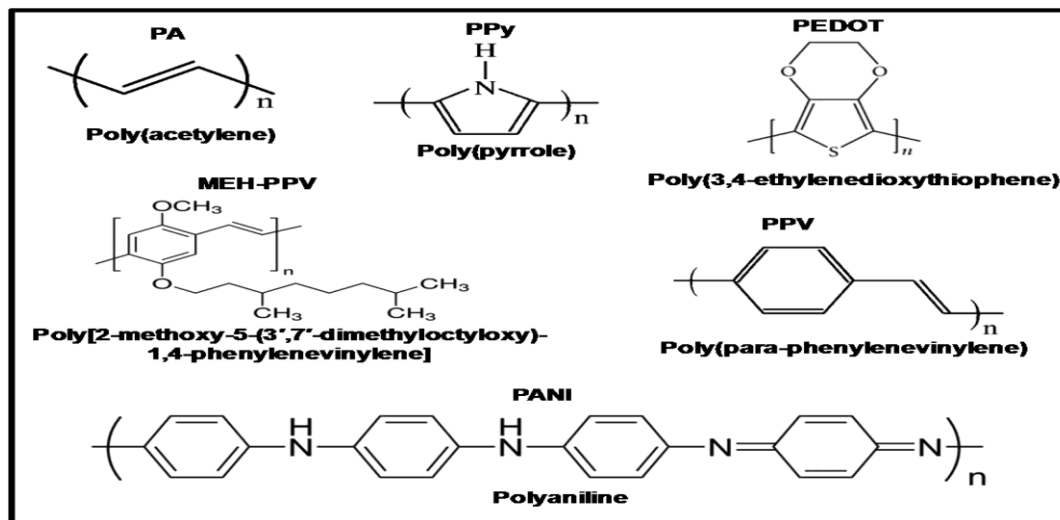


Figure 1. 1 Conducting polymers

For the discovery and development of conducting polymers Alan J. Heeger, Hideki Shirakawa and Alan G. MacDiarmid jointly awarded Noble Prize in Chemistry

Nobel Prize in Chemistry 2000

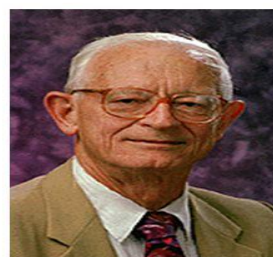
“For the Discovery and Development of Conductive Polymers”



Alan Heeger
University of California
at Santa Barbara



Hideki Shirakawa
University of Tsukuba



Alan MacDiarmid
University of
Pennsylvania

Figure 1. 2 Noble prize winner for conducting polymers

An important CPs is polyacetylene was first synthesized as poly -conjugated linear polymer using catalyst $Ti(OBu)_4-AlEt_3$ by Natta et al, 1957. The polymerization of acetylene was done within broad temperature range -75 to $50^\circ C$ and $100-1140$ torr pressure. High temperature aging of catalyst is foremost important for preparation of conducting polyacetylene films. The structure of monomer acetylene is $H-C \equiv C-H$ polymerizes to form polyacetylene [7]. Polyaniline is another important CP exists in different forms with most common green protonated emerald showing conductivity of $10^5 S cm^{-1}$ much higher than other polymers but lesser than metals i-e $10^4 S cm^{-1}$. The polymerization reaction of aniline was performed in acidic medium where aniline present as cation known as anilinium. Polyaniline can be used in rechargeable batteries; corrosion prevention, LED, Chemical sensors or electro chromic displays [8]. Polythiophene films synthesized by electro polymerization. Polythiophene has attracted much interest because of unique optical, electronic, electrochemical properties. Polythiophene (PTh) is linear polymer of thiophene monomer. The derivatives of polythiophene were synthesized by two German scientists in Bayer's AG

laboratories in 1980. PTh show low reactivity of monomer, low conversion, and infusibility and are insoluble in many of common solvents [9].

Polypyrrole is an organic conducting polymer synthesized by oxidative electrochemical or chemical polymerization of pyrrole. Pyrrole has gained much importance because of its easy synthesis, thermal stability and also it has ability to oxidize via chemical and electrochemical method. Bulky rings in structure of conducting polymers influence largely their solubility. There is widespread misconception that all polymers exist as plastic and insulator in nature[10]. This misconception was cleared by scientists Alan G. MacDiarmid USA professor in university of Pennsylvania, Alan J. Heeger professor in university of California and Hideki shirakawa professor in university of Tsukuba, Japan discovered polyacetylene that has ability to conduct electricity like metal. Hennery Letheby in 1862 discovered polyaniline partially conductive material by anodic oxidation of aniline with sulphuric acid [11]. Poly sulphur nitride, a superconductive material was discovered in 1970s. However discovery of polyacetylene was milestone in the arena of conductive polymers. Polyacetylene was prepared in form of silvery layer with acetylene monomer and Ziegler Natta catalyst in 1974. H. Shirakawa and his co-worker won Noble prize in 2000 for studying electrical properties of polyacetylene. This polymer was prepared in 1974. while these scientist synthesized polyacetylene like a silvery layer using acetylene with Ziegler Natta as catalyst. Regardless of its metal look, in the first shot conductive polymer was not obtained. Whereas in the later three years it was revealed that highly conductive films of polyacetylene can be prepared via oxidation with halogen in vapor phase. The conductivity of polyacetylene films or layers was found considerably higher than some other formerly acknowledged conductive polymer. The discovery of conducting polymer led to the discovery of more organic conducting polymers[12].

1.3 Electrical Conductivity in polymers:

1.3.1 Band theory:

Electronic model is used to explain electronic properties of any material. There are specific or quantized energy levels of electron in an atom according to quantum mechanics. In an atom degenerate energy orbitals overlap to generate molecular orbitals having energy close to each other. Atoms are closely packed in crystal lattice in order to combine and generate molecular orbitals. The highest occupied orbital (HOMO) with valance electrons known as valance band and lowest

unoccupied orbital (LUMO) partially filled or empty known as conduction band. Band gap between VB and CB is small in semi-conductors therefore lower number of electrons having sufficient thermal energy can jump into conduction band [3]. Conductivity of semi-conductors increases with increasing temperature. Band gap between VB and CB is large on insulators therefore valance band is completely filled hence no electron present in CB because electrons do not have enough thermal; energy at room temperature to hoop into CB.

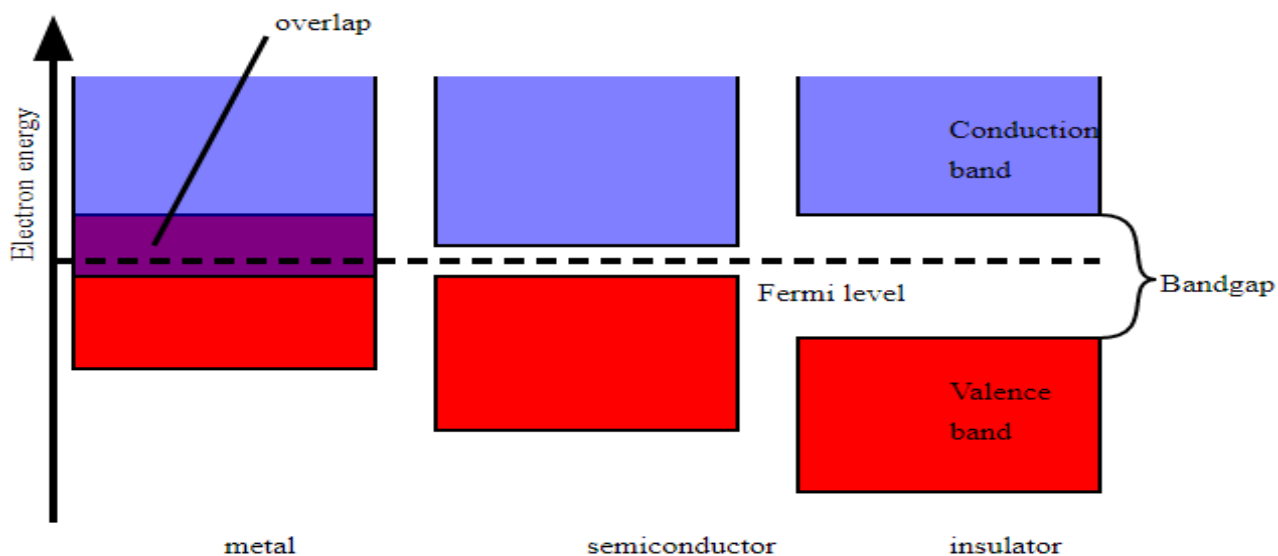


Figure 1.3 Model of band theory

No band gap exist between VB and CB in conductors therefore electrons jump from VB to CB easily resulting high conductivity. Conjugated polymers in their intrinsic state have filled VB and empty CB. For conjugated polymers energy difference between LUMO and HOMO i-e E_g value mostly lie in range 1.5-3.0 eV therefore they are semi-conductors. Doping can change this narrow band gap that involve removal of electron from valence band (p-doping) or adding electron to conduction band (n-doping). In conjugated polymer the removal of electron from HOMO of valence band results in partially filed valence band with generation of free radical cation. The addition of states in band gap from bottom of CB and top of VB results from radical cation (polaron). Removing second electron from chain of positive charge promote lowering of energy

due to generation of bi-polaron.[13] High doping level result in overlapping of localized bi-polarons forming new energy bands in between CB and VB that make flow of electrons easy as depicted in figure 1.4 :

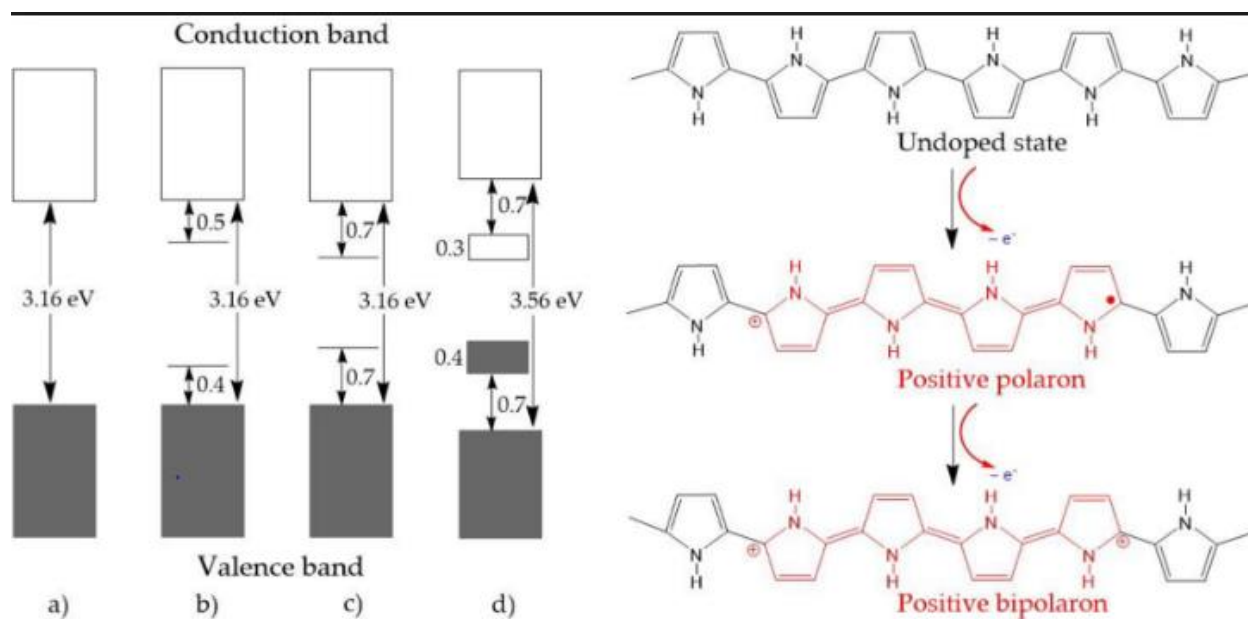


Figure 1.3 Conduction in conducting polymers

1.3.2 Doping in insulating polymers:

Doping can be defined as conversion of insulating polymers into better conductors by increasing conductivity of organic polymers to metallic level either by reduction n-type doping or oxidation p-type doping. In n-type doping strong reductant like sodium naphthalide used as n-dopant to reduce polymer back bone into negative charge carrier. N-dopant lose electron to generate counter cation as a result of doping. Excess of electron presence in polymer backbone make CPs n-type.

In p-type doping polymer lose electron or oxidized by adding oxidant or p-dopant like I_2 , AsF_5 , $FeCl_3$ and electron add up to dopant forming counter anion. Excess of holes will be generated in the backbone of polymer as a result of oxidation that forms CP p-type conductor. Polypyrrole with p-type doping shown in the figure 1.2 in which A like ClO_4^- , Cl^- , NO_3^- act as counter anion.

In doping process complex is generated either by electron acceptor (FeCl_3 , I_2 , AsF_5) in p-type or by electron donor (K or Na) in n-type. The charges either positive or negative appear on polymer chain being doped with counter charged ions are generated by dopant like K^+ , Na^+ , I_5^- , FeCl_4^- . Due to which potential difference will generate that will cause counter ion to jump in and out by putting on electric potential and polymer continue to switch in between conductor, insulator, doped and un-doped state[14] .

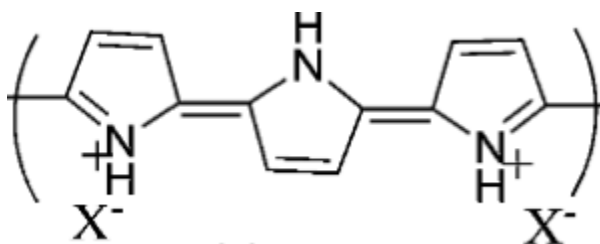


Figure 1.4 Doped Polypyrrole

Doping of CPs does not include replacement of bulky or heavy atom (like Si) with p-type or n-type dopant as in semi-conductors. Doping of CPs includes induction of charges by n-type or p-type doping of polymer chain maintaining neutrality with doping of counter ion. Doping result in change of morphology and volume expansion of CPs.

1.3.3 Bolaron and bi-polaron model:

In CPs like polypyrrole or polyphenylene conduction is due to spin less charge carrying species therefore band theory is not sufficient for explanation of conduction mechanism. Polaron and bi-polaron model is used to explain conduction in CPs. The charges store in the form of polaron and bi-polaron in CPs. Polaron is charge carrier defect state that result in localizing the carrier in potential well generated by deformation of molecules in polymer chain it occupied. The generation of polaron and bi-polaron is determined by level of doping. Low level of doping generate polaron and high level of doping result in bi-polaron. Polaron is the major charge carrier in CPs [15]. In polymer structure polaron is local distortion, formed with removal of electron. Free radical anion or cation are partially localized over various polymer segments. Two types of polaron are present,

one are P- polaron formed by reduction of polymer chain and second one are P+ polaron formed by oxidation of polymer chain. They have $\frac{1}{2}$ spin. Bi-polaron are pair of like charges (like dication) created by coupling of two P- or two P+ polarons in polymer chain. They are spin less and are created as result of large number of polarons on polymer chain. Polaron and bi-polaron are mobile and move along polymer chain. Band theory for CPs given in figure 1.6.

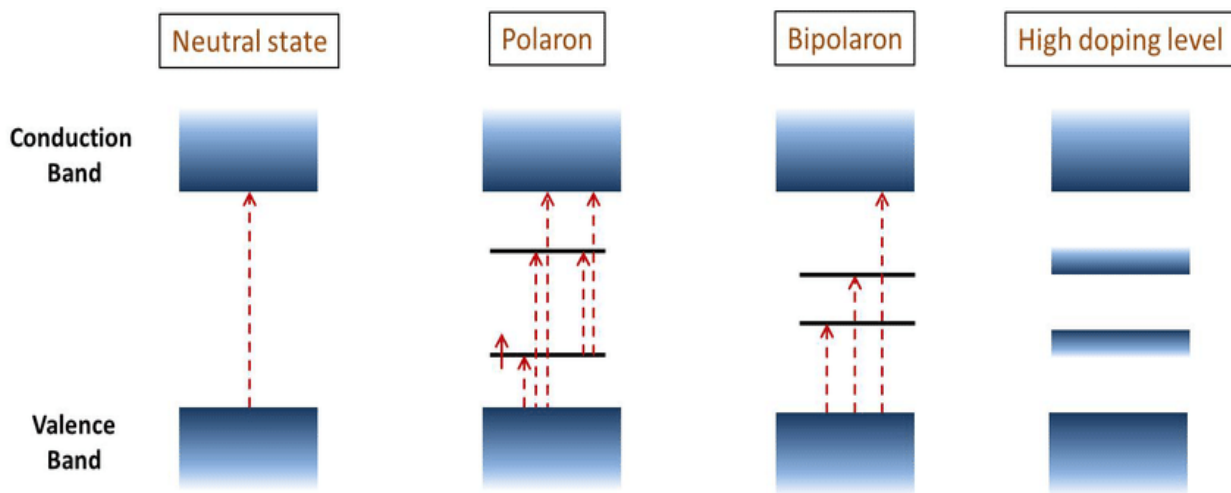


Figure 1.5 Band theory

Production of polaron result by removal of electron from CP generating alteration in polymer backbone. Free radical and positive charge is generated by removal of electron from p system. The subtraction of second electron from valence band create bi-polaron. By further removal of electron or increased in doping continuous bi-polaron generated with increased band gap. At higher doping level upper bi-polaron band combine with conduction band and lower bi-polaron bands combine with valence band producing conductivity like metals [16].

1.4 Polypyrrole as conducting polymer

Polypyrrole is an organic polymer synthesized by polymerization of pyrrole. Pyrrole is five membered ring heterocyclic compound (C_4H_4NH). In various CPs polypyrrole has been studied extensively because of its easy synthesis, higher redox properties, become stable when oxidized, conductivity, and commercial availability, optical and electrical properties. Polypyrrole was formerly called pyrrole black as it was obtained in the form of black powder from oxidative

polymerization of pyrrole monomer. First synthesis of polypyrrole was done in 1888 by oxidative polymerization and electro-polymerization of pyrrole in 1957 to produce polypyrrole. Whereas its conductivity was studied in 1968[17].

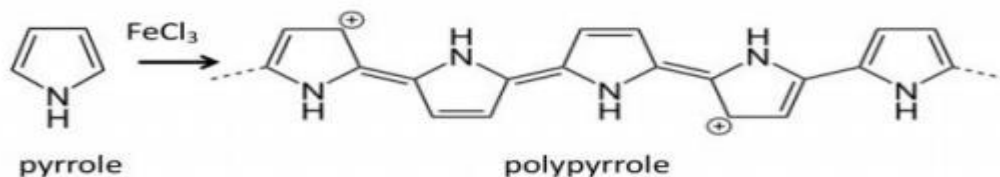


Figure 1. 6 Polymerization of polypyrrole

Conduction in polypyrrole is result jumping of charge carriers i-e polaron and bi-polaron .Band gap in neutral polypyrrole is 3.16 eV. Doping in polypyrrole can result in removal of electron from p-system of polymer backbone forming free radicals and spin less positive charge. The coupling of positive charge and free radical due to resonance result in polaron, generating new localized electronic state. This polaron state in polypyrrole is positioned about 0.5 eV from band edge. With further oxidation polaron combine and replace with new spin less state bi-polaron positioned at 0.7 eV from band edge [18].

With increased doping continuous bands of bi-polaron having increased band gap are finally generated. At higher doping level upper bi-polaron unites with conduction band and lower bi-polaron bands unites with valence band generating conductivity like metals. Polypyrrole exhibit extensive commercial uses because of its composite with good mechanical properties and co-polymer forming nature and electrical conductivity. It is broadly used in super capacitors, corrosion protection, batteries, sensors and radar absorption materials. Polypyrrole is insoluble in organic solvents and show poor mechanical properties due to bulky ring and strong intermolecular interactions present in its structure. This results in limitation of its uses in various fields. Hence researchers are working to resolve this problem by forming blends, composites or by grafting [19].The energy level diagram of polaron and bi-polaran is being represented in figure 1.9 along with neutral chain.

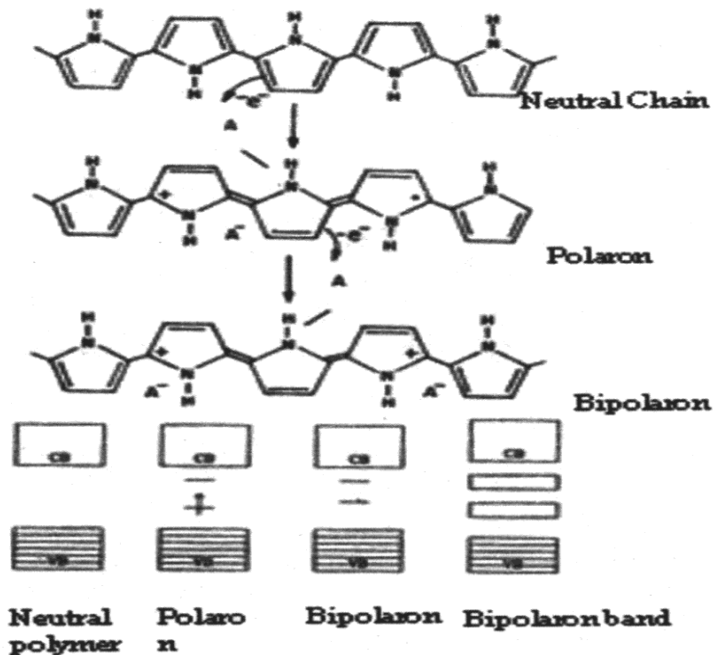


Figure 1. 7 Energy level diagram of (a) Neutral PPy (b) Polaron (c) Bi-polaron

1.5 Synthesis of Polypyrrole:

The synthesis of polypyrrole can be done by chemical and electrochemical polymerization. Polypyrrole is obtained in the form of thin films deposited on electrode via electrochemical synthesis method. This method is complex and product obtained is sensitive to cell conditions, nature and concentration of solvent, concentration of monomer, nature of electrodes, temperature, pH and voltage applied. It can also be synthesized via photochemical polymerization that includes photo irradiation of PPy using photo-sensitizer and via enzyme catalyzed polymerization. These are fast and cheap methods but are not mostly developed ways for PPy synthesis [18].

1.5.1 Chemical polymerization of Polypyrrole:

Chemical polymerization is commonly used for production of polypyrrole due to being inexpensive, fast and simple using no special instrumentation. Polypyrrole in the form of black powder is obtained via chemical polymerization. In chemical polymerization various oxidants are being used like $K_2S_2O_8$, $FeCl_3$ and $Fe_2(SO_4)_3$. Usually oxidant and monomer are dissolved in

solvent at definite temperature [20]. It is a cation radical polymerization as represented in figure 1.10.

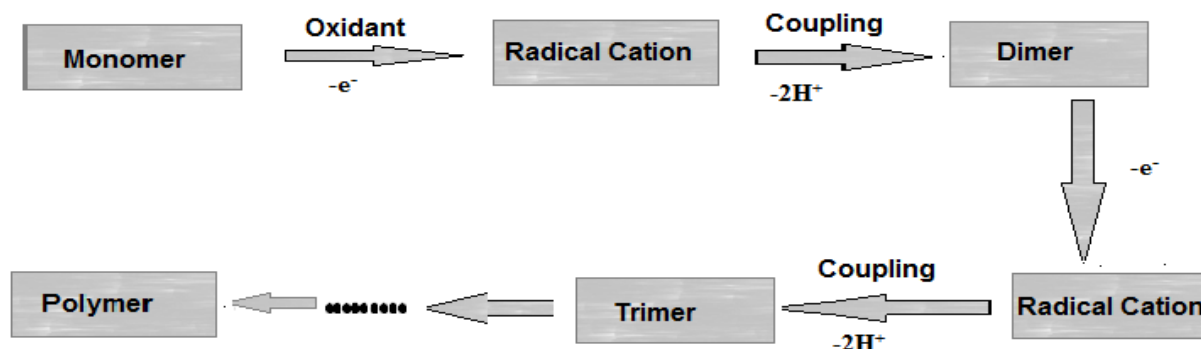


Figure 1. 8 Scheme of cation radical polymerization

In cation-radical polymerization first step is initiation i-e oxidation of monomer into radical cation followed by combination of two radical cation into dimer. Dimer is oxidized to form dimer radical cation. This reaction continues to oligomer formation i-e propagation step. The oligomer ends up into polymer generation followed by termination of chain. PPy is finally filtered, washed and dried. Scheme for polymerization is given in figure. Ferric chloride is the best choice of oxidant in chemical polymerization of polypyrrole. Electro neutrality is maintained by counter anion generated by oxidants during polymerization i-e Cl^- is incorporated as counter ion in case of $FeCl_3$. The chemical polymerization rely on factors like temperature, concentration of oxidant, solvent and time. These factors in affect conduction in polypyrrole i-e conductivity of polypyrrole decrease by increasing temperature. A scheme of chemical polymerization for polypyrrole is shown in figure. Electro-polymerization and chemical polymerization exhibit similar mechanism. First step is oxidation of pyrrole by ferric chloride into radical cation by removal of one electron. This radical cation couple with another radical cation followed by loss of two hydrogen ion to produce dimer i-e (2, 2 bipyrrrole). The reaction continues via continuous re-oxidation of bi-pyrrole to generate chain of PPy. When all monomer is consumed the chain of polypyrrole terminates [21].

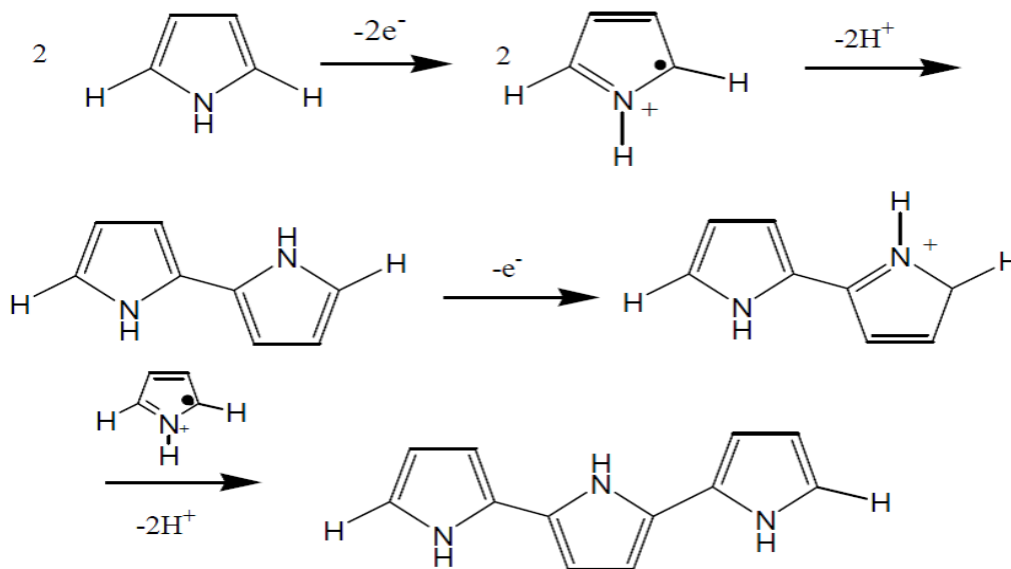


Figure 1. 9 Polymerization of Polypyrrole

1.6 Polymer blends:

A polymer blend can be defined as mechanical combination of two polymers resulting new polymer showing better properties comparative to original one. Polymer blends due to their low prices and eco-friendly nature are talk of the town from previous twenty years. Their properties rely on contents, morphology and properties of each of the individual component taking part in blend formation. Up to now huge number of polymeric blends have been generated having optimal electrical, thermal and mechanical properties [22].

1.6.1 Classification Of polymeric blends:

There are following types of polymeric blends:

1-Miscible blends: Blends of two polymers that are totally miscible into each other showing single phase structure are miscible blends. They show one glass transition temperature. Example is poly (propylene oxide)/polystyrene.

2-Immiscible blends: These blends show more than two phases with poor adhesion having large domain of dispersed phase. They have two glass transition temperature. Examples are poly (propylene oxide)/polyamide and acrylonitrile butadiene styrene/polyamide etc.

3-Compatible blends: The immiscible blends having strong interface interaction between polymer blends components are compatible blends. They show morphologically uniform physical properties whereas show in-homogeneity on smaller scale[23].

4-Compatibilized blends: The immiscible blends into which surface active species or compatibilizers are used to stabilize their physical properties [24].

1.6.2 Methods of blending:

The formation of blends is not spontaneous process as most of polymers are immiscible into each other. Most common methods used for blending are solution blending, melt mixing, graft copolymerization or latex mixing. Melt blending is commonly used method for polymeric blend formation which includes mixing of two polymers that are in molten form in batch mixer or extruders in order to get homogeneous polymeric blend. This method show some limitations i-e consumption of high energy. Solution blending method comparative to melt blending is mostly used at laboratory level. It is a simple method that includes blending components in suitable solvents. Both components of blends are dissolved in common solvent i-e chloroform, DMSO, THF or DMF with constant stirring. Solvent is evaporated to get pure polymer blend [25].

Solution blending is better than melt blending as it includes fast mixing and low consumption of energy. These days a fresh method is used for polymeric blend formation i-e solid state shear pulverization or cryogenic mechanical alloying. In this technique below melting temperature polymers are grind together using twin screw mixer that creates repeated polymer fragmentation. This provide nano-scale blends[26].

1.7 Copolymer:

Polymers showing required properties can be synthesized by mixing two or more monomers to create copolymer. The order of monomers rely on their relative reactivity. It can be alternating or

random. Block copolymer can be synthesized via various polymerization methods. They do not exist naturally [27].

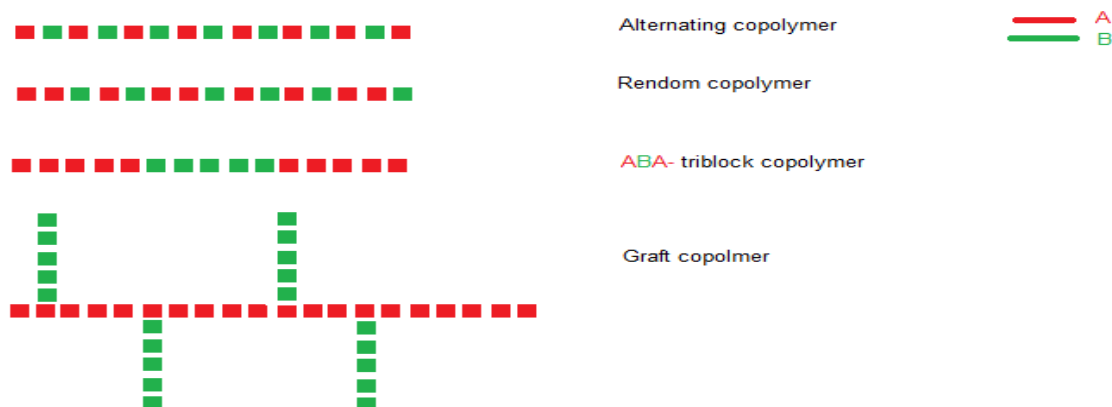


Figure 1. 10 Types of copolymer

Monomers can be linked in different ways like ABA tri-block copolymer that contain long block of monomer A following block of monomer B and at both ends linked with two A blocks. Firstly ABA type block copolymer was synthesized by adding propylene oxide to ethylene oxide containing propylene oxide that is hydrophobic and ethylene block that is hydrophilic. In aqueous medium it form micelles with core hydrophobic and outside oriented hydrophilic part. Examples for ABA type block copolymer are polystyrene-block-polyisoprene-block-polystyrene, polystyrene-block-polybutadiene-block-polystyrene etc. These were studied as thermoplastic polymers [28]. Firstly these were obtained as derivative of plasticized PVC and were named as Plasticsols[29]. The distinctive hard and soft phases were present in thermoplastic elastomers. Soft fragments are amorphous whereas hard fragments are crystalline in nature. In SIS copolymer isoprene is soft and amorphous fragment while styrene is hard and crystalline fragment. Copolymers containing polymers with diverse properties cannot be separated into individual constituents i-e styrene and meth-acrylic acid containing block copolymers. These have good solubility in polar and non-polar solvents. Acrylic acid constituent is coiled in non-polar solvent whereas extended in polar solvent. Each constituent in block copolymer show its own striking features and have specific glass transition temperature[30].

1.7.1 Structure and properties of SIS copolymer:

Polystyrene-block-polyisoprene-block-polystyrene or SIS is an example of ABA type block copolymer containing macromolecules i-e polystyrene block covalently bonded to polyisoprene block[31, 32]. This copolymer exhibit high elasticity, flexibility with glass-rubber-glass kind of configuration in which rubber section provide flexibility as both ends of rubber sections are connected to glass section that makes SIS copolymer as mechanically helpful elastomer[28]. Soft and hard fragments in SIS block copolymer represented in figure 1.13.

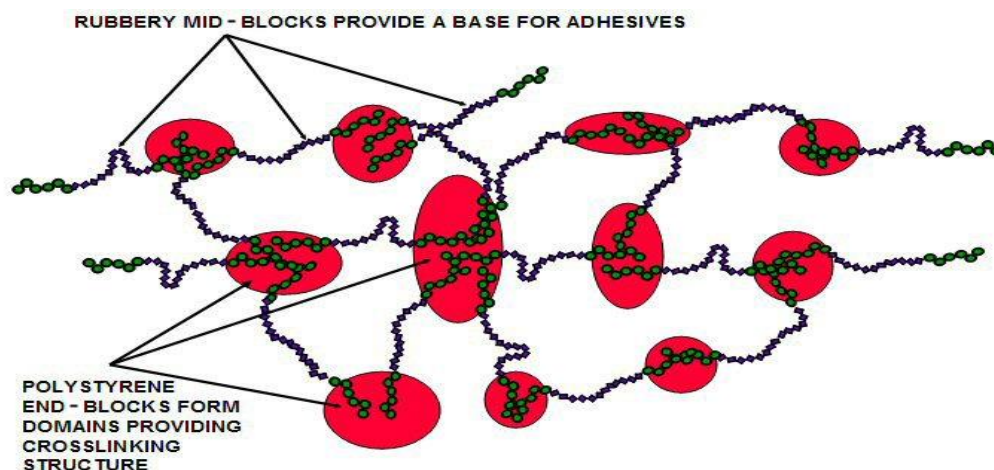


Figure 1.11 SIS block copolymer

Poly-isoprene is synthetic form of natural rubber having rubbery, flexible and soft nature. Whereas polystyrene is synthetic transparent polymer prepared polymerization of monomer i-e styrene. It has low melting point and it is glassy at room temperature showing thermoplastic nature. It flow if heated above T_g i-e glass transition temperature[33]. Polystyrene is brittle, hard and rigid. It form semi-crystalline phase which provide strength to copolymer. I shows low resistance to oxygen and water vapors. In copolymer rubbery poly-isoprene portion act as elastomeric. If copolymer is heated above T_m i-e true melting temperature of PS block whole chain become mobile and if cooled PS block reforms[34].The structure of SIS polymer being shown in figure 1.14.

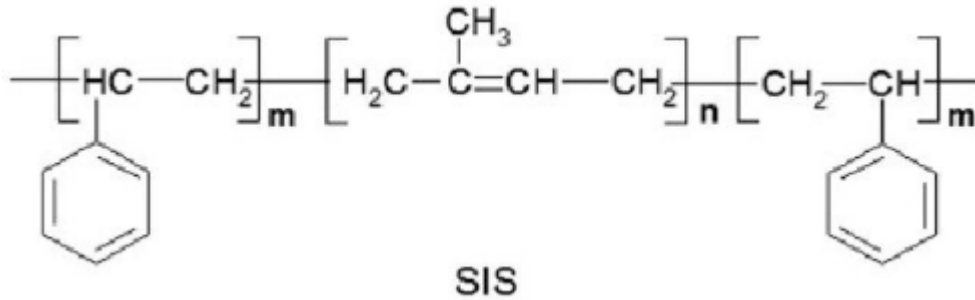


Figure 1.12 Structure of SIS copolymer

SIS show excellent film making properties because of its elasticity and provide enhanced features like better processibility and compatibility. It is adhesive on textured materials like corrugated paper, wood or to wear out labels that are impossible to remove therefore it can be cast off as pressure sensitive adhesives. Poly SIS is soft and by increasing styrene content its modulus can be increased. Whereas with increase in styrene content its elasticity and recovery properties get worst. Therefore there should be optimization for modulus and elasticity. Poly SIS show solubility in organic solvents i.e. 7.7 and 9.4 delta in solvents like THF or chloroform etc. It is used as electrical insulators because of poor electrical conduction[35].

1.8 Nanomaterial:

Nanotechnology is a fast developing field of producing materials at nano dimensions where nano is one-billionth of a meter. Nano-materials show one or more dimensions in a scale range of 1-100 nanometer[36]. They exhibit unique properties comparing to the same material at bulk. Nano-materials are categorized into four types depending on dimensions:

1. 0D nano-materials have all dimensions in nano-scale range (1-100nm) or no dimension greater than 100nm. For example fullerene, nano-powder or nano-particles etc.
2. 1D nano-materials have at least one dimension greater than 100nm. For example platelets, thin films or surface coating etc.
3. 2D nano-materials have at least two dimensions greater than 100nm. For example nano-wires, nano-tubes or dendrites etc.

4. 3D nano-materials have length greater than 100 nm in all of three dimensions. For example colloids, quantum dots or nano-crystals etc [37].

The nano-materials show enhanced surface area to volume ratio that results in greater number of active sites in nano-particles comparative to bulk material. Therefore nano-materials can be used in extensive range of fields like energy storage, medical, industry, clothing industry and cosmetics etc[38].

1.8.1 Different approaches for Synthesis of nano-particles:

The variety of techniques have been used for synthesis of nano-particles. Two major techniques being used to prepare fine nano-particles are bottom-up and top-down approach represented in figure 1.15[39]. In bottom-up approach building blocks of atoms or molecules self-assemble to create nano-particles. This is a most common used technique for production of nanoparticles that generate particles with uniformity in size distribution having same geometry and higher flexibility. Using this technique monometallic or bi-metallic both type of nano-particles can be produced biologically or chemically. On the other hand in top-down approach external force is applied on bulk material to break down into nano-particles. This technique involves attrition, ball milling or repeated quenching. Top-down technique has some constraints like varying geometry with broad size range distribution. A chance of contamination is there in case of ball milling[40].

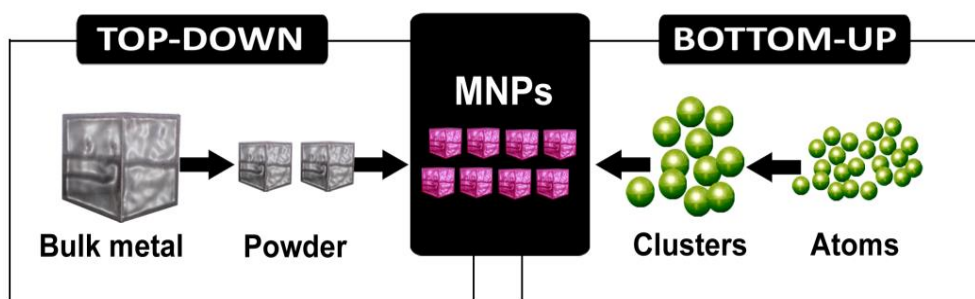


Figure 1. 13 top-down and bottom-up approach for synthesis of nano-particles

There are various chemical procedures like alcohol reduction or sono-chemical. These procedures show some restrictions like toxic chemicals absorb on the surface of nano-particles. Nano-particles can also be synthesized using green chemistry i-e via biological techniques that involves use of

enzymes, fungi, bacteria, micro-organism and extract from plants. This technique is good for environment reducing use of harmful chemicals. The green method involves ecofriendly solvents, reducing agents for complex formation with metal and capping agent for controlling size of particle[41].

Researcher are working to invent new environmental friendly techniques to produce nano-particles. Example includes B2 vitamin that is used as reducing as well as capping agent in synthesis of nano-particles. It is less harmful comparing to other reducing agents i-e NaBH_4 (sodium borohydride) being used in chemical techniques. Green reducing agents i-e B2 vitamin form metal complex via reducing metal oxides to nano-particles and also cap with oxidized B2 vitamin[42, 43].

1.9 Nano-composites:

Nano-composite is a material prepared by joining two phases that contains at least one phase with nano-scale dimensions. Nano-composites comprise of various classes but generally large phase is called matrix whereas phase embedded in matrix is called reinforced phase. If nano-fillers are used as reinforced phase properties of matrix phased can be enhanced. Nano-composites can be used as alternatives to micro-composites because of enhanced magnetic, electrical, optical and mechanical properties. Due to reduced size of nano-fillers nano-composites show high surface to volume ratio[44]. Reinforced phase can be nano-particles, carbon nano-tubes, nano-sheets, nano-fibers or minerals. While synthesise of nano-composites elemental composition control is an issue. Carbon nano-tubes discovered in 1991 being used as reinforced phase in nano-composites. Natural occurring nano-composites are bones comprise of 30% matrix i-e collagen or 30% nano-minerals i-e crystal of hydroxyapatite[45].

1.9.1 Classification of nano-composites:

Depending on matrix and reinforced phases nano-composites can be grouped in to different classes i-e carbon nano-tubes reinforced nano-composites, nano-clay reinforce nano-composites, inorganic particles reinforced nano-composites and nano-fiber reinforced nano-composites[44]. Depending on matrix nano-composites are categorized into three categories:

- **Metal matrix nano-composites:** These are composed of metal or alloy as matrix phase with nano-particles as reinforcement. Metal matrix nano-composites show excellent mechanical, physical and chemical properties. They can be prepared by number of ways like vapor deposition method, sol-gel method, rapid solidification and spray pyrolysis etc. For example: Ni/Al₂O₃, Fe-Cr/Al₂O₃, Mg/CNT etc[46, 47].
- **Ceramics matrix nano-composites:** These are composed of ceramic material i-e nitrides, silicate or nitrides as matrix phase. These nano-composites exhibit large range of applications because of their extraordinary mechanical and electrical properties. There are various techniques used for synthesis of ceramic based nano-composites i-e polymer precursor route, sol-gel method, template method or spray pyrolysis etc. Examples are Al₂O₃/CNT, Al₂O₃/SiO₂ or Al₂O₃/TiO₂ etc[48, 49].
- **Polymer matrix nano-composites:** These contain polymer as matrix and nano-additives as reinforcement. These nano-additives can be 1D i-e nano-tubes, 2D i-e nano-clay or 3D i-e quantum dots. Carbon or glass fibers are reinforcements in polyamide polymer. Nano-fillers are used in number of sizes and configurations that can be plate like, tube like or 3D particles. Polymers shows bad mechanical or electrical properties that can be improved via nano-composite formation. Polymer matrix mostly have weak or poor interaction with filler constituent or in some cases chemical bond in nano-fillers and matrix exhibit distinctive anisotropic geometry showing enhanced mechanical properties[50].

Polymeric nano-composites can be prepared via sol-gel method, melt mixing, template synthesis or in-situ polymerization etc. The features of nano-composites relate to filler being used, rate at which two phases are being mixed, morphology of nano-fillers and volume fraction of nano-particles. The dispersion of nano-fillers should be uniform or agglomeration will occur resulting nano-composites with poor properties[51].

1.9.2 Applications of polymeric nano-composites:

Nano-composites show wide range of applications in various fields because of enhanced electrical, optical, magnetic and mechanical properties. Toyota motors prepared nylon6/ mont-morillonite polymeric nano-composite that was used to make belt cover in car model[52]. Polymers exhibit bad electrical conductivity and resistance to fire nano-clay reinforcement delay melting point

improving fire resistance. It also reduce air diffusion in polymer[53]. These clay/ polymeric nano-composites find application in submarines, vehicles and aero planes to avoid risk of fire. Researcher have stated properties like microwave absorption for polymeric nano-composites having iron oxide, tin oxide, titanium oxide as nano-fillers. Due to high Young's modulus and hardness polymeric nano-composites i-e clay/PP show scratch resistance[54]. Conjugated nano-composites been stated as biosensors and gas sensors. Large flexible solar cells been made out of polymeric nano-composites[55].

1.9.3 Nano-composites fabrication method:

The assembly of nano-composites involves unvarying dispersal of nano-particles in polymer matrix as nano-particles usually show agglomeration that limits dispersion in matrix. Commonly three techniques being used for uniform dispersal of nano-particles. First technique being used is solution blending, second is direct mixing of polymer matrix and nano-particles and the last one being used is mixing of nano-particles with pre-made polymer matrix[56].

- **Solution blending:** This technique is commonly used to fabricate nano-composites. It includes dispersal of nano-particles with polymeric matrix in appropriate solvent. Firstly polymer is being dissolved in appropriate solvent then mixed with nano-fillers mostly at room temperature. The mixture is added in petri dish and solvent is evaporated. Nano-composite is attained as film. It is the simplest technique at laboratory level but challenging at industrial scale as large quantity of solvent being used[57].
- **In-situ polymerization:** In this technique, firstly nano-fillers are dispersed in solution of monomer following polymerization. Polymeric matrix grafts on the surface of nano-particles. The low molecular weight monomer seep into the layers between nano-fillers resulting swelling of nano-fillers. This solution is polymerized using heat, radiations or any organic initiator. The monomer get polymerized forming intercalated type nano-composites. Numerous polymeric nano-composites have been generated via in-situ polymerization like nano-tube/PPy nano-composite, MWCNTs/PPy nano-composites or nano-tube/ PPy nano-composites[58].
- **Melt intercalation method:** This technique is being used at industrial level to fabricate nano-composites. It includes mixing of nano-clay or nano-particles at melting

point in order to anneal the reaction mixture. In this method melting of reaction mixture to viscous liquid is followed by adding nano-fillers at high temperature diffusion and shear. By compression molding nano-composite get its final shape. Risk of agglomeration of nano-fillers is there that have to be overcome using solution blending technique[59].

Chapter 2

Literature review:

2.1 Green synthesis of nano-particles:

The researchers have used numerous plant extracts for production of nano-particles as this method is environmental friendly. Plant extract contain reducing agents that form complex with metal atoms and reduction of metal salts resulting nano-particles that are also capped for stability[60].

Vinod V. Thekkae and M.Cemik used gum karaya for synthesis of cuo nano-particles. The average size of nano-particles found to be 7.8-4.8nm using TEM. The confirmation of cuo nano-particles was done via FTIR, XRD and XPS analysis. Nano-particles were found to be single-phase monoclinic structure. Cuo nano-particles were used to study anti-bacterial properties. E.coli and S. aureus was worked out and found that cuo particle being synthesized from gum karaya show high level of anti-bacterial activity[61].

Sangeetha Nagrajan and Kumaraguru synthesized zno nano-particles using sea weed extract i-e brown myriocystum, red Hypnea Valencia and S. myriocystum. The initial testing showed that s.myriocystum sea weed extract succeeded to produce zno nano-particles. The extract of S.myriocystum contain fucoidan that is water soluble and result in reduction of zinc oxide nano-particles. The characterization was done via TEM, XRD, SEM-EDX, AFM and FTIR. The average size found to be 36nm. These green synthesized nano-particles were used for anti-bacterial against gram-positive bacteria[62].

Umesh K. Parida, P. Nayak and Birendra k. Bindhani use onion extract for synthesis of gold nano-particles. The research found to be cost effective and friendly to environment. The extract of allium cepa was used as reducing agent due to presence of vitamin c in its extract. Nano-particles were

characterized via XRD, TEM, UV-visible and SEM analysis. The nano-particles found to be polydispersed as absorption peak appear at 540nm that broaden with increase in time. The internalization with in cell relating nano-particles was studied and found to be effective[63].

Seema sharma and Naheed Ahmad worked out silver nano-particles using extract of ananas comosus. For characterization HRTEM, UV-Visible spectroscopy, EDX and selected area diffraction pattern (SAED) was used. The nano-particles found to be spherical with average size 12nm. Antioxidants i-e phenols present in pineapple are used as reducing agent for Ag metal ions. Nano-particles thus produced remain stable for 4 month incubation[64].

X.G Fuku, N.Mayedwa and M.Maaza produced zno using extract of Morunga oleifera as reducing agent. The nano-particle was characterized for morphology, crystalline structure, isothermal behavior, electrochemical activity, composition and optical properties via CV, XRD, HRTEM, SEAD, FTIR, DCS /TGA and UV-Visible spectroscopy. The nano-particles with average size 12-30.5 nm was synthesized. Phytochemicals i-e flavonoids or vitamins are chelating agents[65].

2.2 Polypyrrole blends:

Polypyrrole is insoluble, brittle and show poor processibility. It do not possess any mechanical properties because of strong intermolecular bonding and bulky ring in structure that shorten its uses. The thermal, electrical and mechanical properties of polypyrrole can be enhanced by making blends with appropriate thermoplastic polymers. Making blends is best way to get polymer showing better properties. By making blends of insulating polymer brittleness can be controlled and high level of processibility can be achieved[66, 67]. V.Mano and co-workers produced blend of polypyrrole with PVC and worked out electrical, thermal and mechanical of these blends. These blends were produced via chemical polymerization of polypyrrole and adding PVC with FeCl₃ to vapors of polypyrrole for about 2 hours and 6 hours at room temperature. Synthesis of blends was assured via FTIR analysis. Researchers worked out that for blends, Young's modulus affected by FeCl₃ concentration and time of exposure. Cyclic voltammetry was used to work out electrochemical properties that show variation from 10⁻⁴ Scm⁻¹ to 10⁻¹ Scm⁻¹. Thermal behavior of polypyrrole blend does not show any change[68].

M. Omastova synthesized blend of polypyrrole with polypropylene via melt blending method and worked out change in electrical, mechanical and thermal properties of polypropylene. It was

studied that increasing polypyrrole content increased mechanical, thermal and electrical properties of blend. Four point probe technique used for study of electrical conductivity and was found to be enhanced comparative to pure polypropylene. The dispersion of polypyrrole in polypropylene was enhanced via sodium dodecyl-sulphate and improvement in thermal, electrical and mechanical properties[69].

Hsing-Lin and co-worker Jack E.Fernandez prepared blend of polypyrrole with poly (vinyl methyl ketone) via electrochemically and chemical technique. The increase in threshold conductivity up to 10 % was reported with increase in concentration of polypyrrole concentration. Blend formation confirmation was done by FTIR. The crystallinity does not depend on PPy concentration was confirmed by XRD analysis. Blends stability was measured by TGA and blends obtained via chemical method show stability up to 325⁰ C whereas stability up to 280⁰ c was shown by blends obtained from electrochemical method[70].

S.Hosseini hosseini and Ali Entezami synthesized blend of PPy with Various insulating polymer including PVC, PS and PVAc and worked out sensing behavior of these blends for numerous poisonous gases. Their synthesis confirmation was done using FTIR. Four point probe method was used for study of electrical conductivity[71].

Hsing LIN and co-workers synthesized blends of PPy and Polythiophene with insulating polymers that insulating polymers that include PS and polycarbonate resin. Threshold conductivity was reported at 18 weight % concentration of two conducting polymers with polystyrene whereas at 12 weight % in case of polythiophene/polycarbonate blend. The low value was due to homogeneity as result of hydrogen bonding [70, 72].

2.3 Polymeric nano-composites:

Comparison study was done to check the increase in mechanical strength using graphene and nano tubes as reinforcing phase. Models were prepared with same percent weight of both reinforcing phases. Mechanical properties were determined by using pull out and strain constant method by measuring the van der Waal forces or other interacting forces between polymer matrixes and reinforcing phases. The experimental results show increase Young's modulus, tensile strength. Graphene does not allow the increase in formation of cracks or delayed crack formation comparing to nano tubes. Molecular dynamic simulation was performed to compare mechanical properties

enhancement of polymer nano composites i-e graphene nano sheets/polymer or Nanotubes/polymethylmethacrylate [73]

Synthetic method for polymer nano composites using multi walled carbon nano tubes (MWCNTs) was developed in this research work and their mechanical strength was calculated. Modification of surface of MWCNTs using acid. An emulsion was prepared using surface modified multi walled carbon nano tubes and liquid monomer benzyl methacrylate. These modified MWCNTs largely affect the composite particles size and surface coverage. Hence due to better interaction mechanical strength was increased as MWCNTs proved to be good nano filler in polymer matrix[74].

Polymer nano composite with silica as reinforcing phase and polymer matrix was prepared. The constant strain method was used to calculate elasticity of composite. The molecular dynamic simulation was done to study increase in tri-biological properties i-e wear and tear, friction etc was checked by using iron as top layer of polymer nano composite. Experimental results clearly showed increase in young's modulus and decrease in friction and abrasion by the addition of silica nano particles as filler in polymer matrix. To know about the reasons for the increased tri-biological properties the interactions between the reinforcing phase i-e silica and polymer matrix, concentration of atoms in polymer composites and radius distribution factor was studied and determined[75].

Polymer composites with original and modified graphene as reinforcing phase was prepared and studied for increased tribological properties. The interactions between polymer matrix and reinforcing phase were studied by pull out method. By sliding iron as upper layer on polymer surface friction and abrasion study was done. Molecular dynamic simulation was performed that showed decrease in friction and abrasion rate with modified graphene. In order for detailed study of mechanism for tribological properties enhancement the interacting forces, energy and radius distribution factor was studied and calculated. In this research work, one can get good understanding about mechanism responsible for increase in tribological properties of modified MWCNTs [76].

Titania nano particles can be used as reinforcing phase in polymer matrix increasing mechanical strength. These nano composites work in hydrothermal conditions or not are yet to be tested. In this work the influence of Titania nano particles was studied on thermal properties, strength and

sorption of water. For particular amount of titanium reduction in water diffusion, increase in flexural strength and shear strength was observed. The increase in mechanical strength of polymer nano composites in hydrothermal condition can result in creation of variety of options for development in engineering. Weibull model was used for stress-strain curve evaluation and showed similar result to experimental results[77, 78].

The addition of nano particles as reinforcing phase or filler enhances the mechanical strength of polymer nano composites. In this research polymer nano composite was prepared using melt blending method containing aluminum nitride (cheap, stable structure of crystal and with greater mechanical strength) as reinforcing phase and thermoplastic polymer matrix i.e high density polyethylene. Nano indentation process was used to measure mechanical properties of polymer nano composites. For surface morphology atomic force microscopy was used. The structure at micro level was studied by X- ray diffractometer, Field emission gun-scanning electron microscopy and high resolution –tunneling electron microscopy. The characterization showed uniform dispersion of aluminum nitride in polymer matrix. With increase of concentration of nano particles increase in mechanical strength was observed[79].

In this work chitosan i.e linear polysaccharide as polymer matrix and zinc oxide nano particles as reinforcing phase was used to prepare polymer nano composite for the very first time. These polymer nano composites were analyzed using physical and chemical techniques. Dielectric constants and conduction properties were studied. Due to addition of zinc oxide nano particles dielectric constant and conduction properties of polymer nano composites increased. These polymer nano composites were tested for antimicrobial activity. The study showed increase in the efficiency of these composite layers or films against microbes comparative to original or pure chitosan. Mechanical strength increased due to zinc oxide nano particles. About four films were prepared and tested for dielectric constant, electrical conductivity, anti-microbes and mechanical strength[80].

Polymer nano composites with hydroxyapatite as reinforcing phase and high density polyethylene as polymer matrix were prepared using two different methods. Firstly polymer nano composites were by grinding in mixer granular sample of high density polyethylene and hydroxyapatite using different concentration of hydroxyapatite i.e reinforcing phase. In second method powdered form of hydroxyapatite using different concentration added to solvent whereas polymer matrix i.e high

density polyethylene was prepared using xylene at boiling point in the form of powder at nano scale. For characterization thermal properties, mechanical strength and morphology was analyzed. Experimental results showed better results for powdered polymer nano composites than those of granular because of good distribution of reinforcing phase into polymer matrix. In granular and powdered composites increase in cross linking observed with increase of hydroxyapatite nano particles concentration by gel content and hot set tests[81]

For the enhancement of mechanical strength of polymer matrix silicon carbide nano wires were added to the polymer matrix using method i-e in-situ growth method. Silicon carbide nano wires were produced on carbon fiber's surface and within polymer matrix. Silicon carbide nano wires prepared by this method can strengthen carbon fibers and increase mechanical strength of polymer nano composites. Silicon carbide nano wires acting as reinforcement as well as increasing bonding between two phases[82]

Graphene nano materials used as reinforcing phase in acrylonitrile butadiene polymer matrix. The addition of certain amount of graphene reinforcement increased tensile strength was analyzed comparative to pure polymer matrix. Graphene nano materials were used combined with carbon black and multi walled carbon nano tubes and used as reinforcing phase showed better results than graphene materials used alone as reinforcements using same load. In these hybrid reinforcements better results with graphene nano materials and carbon black comparative to MWCNTs for increased mechanical strength and stability against heat as well as good electrical conduction. Tensile strength and break resistance was observed up to certain concentration[83]

This work involves MWCNTs as reinforcing phase. Firstly these were modified by treatment with acid and plasma. Melt blending method was used for polymer nano composite preparation, polymer matrix used is polyetherimide. From previous study it was noticed that hybrid reinforcement i-e graphene nano materials with carbon black show better reinforcement as compare to MWCNTs hybrid with graphene nano materials. Hence modification is done. Polymer nano-composites with certain amount of functionalized MWCNTs results in enhanced mechanical strength comparative to pure polyetherimide. The model namely Coats-Redfern was used for thermal properties analysis. Betterment in thermal properties was observed with reinforcing phase. Due to surface modification adhesion properties within polymer matrix and nano particles

improved due to uniform distribution of reinforcing phase observed by characterization techniques including FT-IR and SEM[84].

This research involves the effect of nano materials i-e graphene or carbon materials at nano scale on the structural morphology and mechanical strength of polymer matrix i-e hydrogels by analyzing the distribution of nano particles in water medium and interaction of these nano materials with hydrogels. The main light is on procedure used for synthesis, mechanical properties and structural morphology of polymer matrix along with interactions and effect of structure on properties. The properties of nano materials and synthesis or fabrication methods are defined along with their pros and cons. This work highlights recent trends for using nano materials with hydrogel effectively. The products of this work can be helpful to engineers and scientists[85].

Geo-polymer (prepared in alkaline media from alumino silicate) used as polymer matrix and clay platelets at nano scale as reinforcing phase used to study their influence on mechanical strength and thermal behavior of polymer matrix. These clays are nowadays being used as replacement for traditional cement therefore seeking lot of interest for research. Different weight percentages of nano clay being added to polymer matrix. The characterization is done by XRD, FT-IR and SEM. The increase in mechanical strength is observed due to addition of nano clay to polymer matrix. The addition of certain quantity of nano clay result in reduced porosity and decrease in water absorption capacity of composite. Nano clay enhances flexural strength, hardness and compression strength. Nano clay act as reinforcing phase as well as help in polymerization reaction for geo-polymer[86].

The mechanical strength and biocompatibility for composites of graphene nano materials and alumina ceramic is being studied. Using different graphene nano material concentration alumina ceramic was prepared and sinteration was done in furnace under controlled conditions. Density of ceramic composite varies for certain quantity of graphene platelets. Mechanical strength was increased by addition of graphene nano materials in alumina matrix. Biocompatibility test also showed positive results. The biocompatibility and high mechanical strength seeks interest in various fields of science and technology[86]

Graphene as reinforcing phase for polymer matrix used to prepare polymer nano composite and studied for mechanical strength and tribological (friction and abrasion) properties analysis. Mechanical properties i-e young's modulus and shear strength is calculated using strain constant

process. For tribological properties i.e friction and abrasion rate determination model is prepared with iron as upper layer on polymer matrix .Molecular dynamic simulation was done that conclude increase in young's modulus, hardness and shear strength. Friction and abrasion rate decreased by addition of graphene nano materials [76, 87]

Motivation:

The increase in mechanical strength of polymer is comparatively higher at nano scale than large scale reinforcement. In current research scientist have work hard to develop polymer reinforced by nano particles and have obtained good results. The increase in mechanical strength can be improved by maintaining the fine dispersion of nano-particles within the polymer matrix and by the modification of the surface of nano-particles that act as reinforcement phase. The green synthesis of nano-particles using plant extract has gained considerable attention because of minimal use of harmful chemical solvents. In this research work V_2O_5 nano-particles were synthesized using green tea extract with no hazardous reducing agents and stabilizing agents. The polymeric nano-composites of Poly S.I.S-PPY/ V_2O_5 with enhanced mechanical properties was prepared that found its profound applications in industries like EMI shieldings.

Chapter 3:

Experimental

3.1 Materials:

The precursors used in research work are Ammonium meta-vanadate (NH_4VO_3) purchased from Merck. Anhydrous iron (iii) Chloride used as oxidant purchased from Sigma Aldrich. Pyrrole was obtained from Fluka Bio-chemika and its distillation was performed before use. Acetone and ethanol were purchased from Fluka and used for washing. Deionized water obtained from Vitro diagnostic laboratory Islamabad. Poly SIS tri-block copolymer was purchased from Sigma Aldrich.

3.2 Green synthesis of nano-particles:

The use of chemical methods for synthesis of nano-particles have several disadvantages like

Expensive chemicals, Toxic chemicals, poisonous by-product and long reflux time. Green synthesis has earned importance because of environment friendly nature and low cost[88]. In current research work green tea i-e *Camellia Sinensis* being used for preparation of nano-particles.

3.2.1 Composition of green tea (*Camellia Sinensis*):

The reduction of nano-particles using camellia sinensis has earned importance recently. Green tea leaves have high content i-e 30 % of catechins or polyphenols. Green tea leaves also have 7% carbohydrates, 7% lipids, 4% amino acid, 15% proteins, vitamins C and D. Catechins or polyphenols show antioxidant properties used to reduce metal ions into nano-particles that are also capped and stabilized via lipids, amino acids, or proteins hence there is no need of external capping agent or surfactant to stabilize nano-particles. Six main catechins present in green tea leave extract are (-) epicatechin-3-gallate (ECG), (-) Epigallo-catechin (EGC), (-) Epicatechin (EC), (-) Epigallo-catechin-3-gallate (EGCG), (+) Gallo-catechin (GC) and (+) Catechin represented in figure 3.1[89].

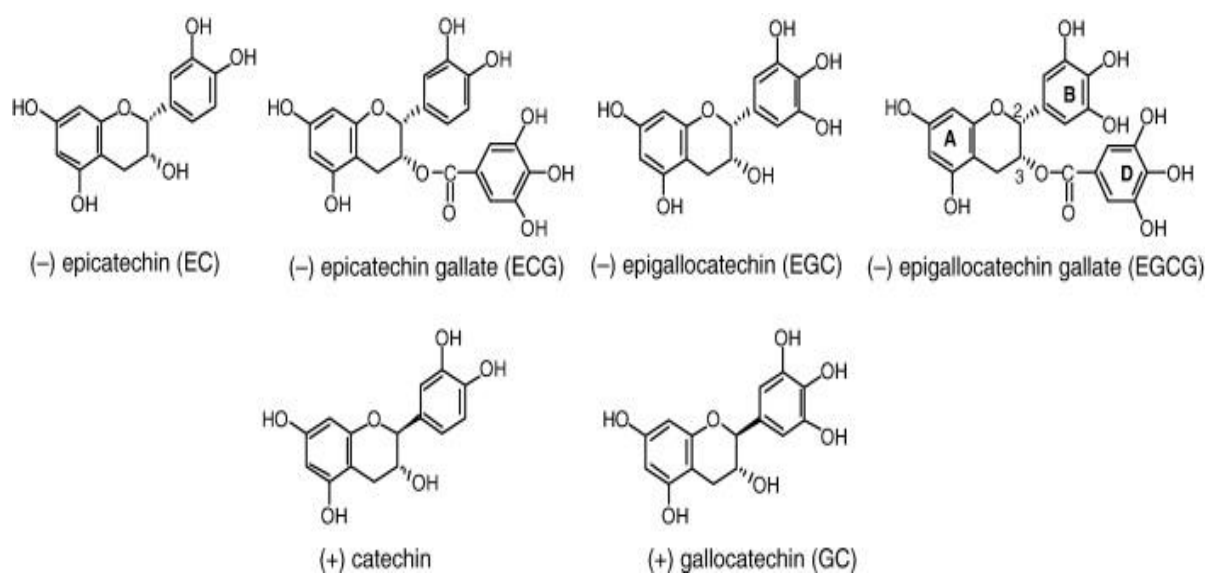


Figure 3. 1 Phenolic catechins in green tea leaves

3.2.2 Preparation of green tea extract:

Green tea extract was prepared by adding 2g of green tea leaves in 100mL deionized water in conical flask. Then mixture is boiled for 30 min at 65⁰C and filtered in ordered to get extract.

3.2.3 Preparation of vanadium penta-oxide nano-particles:

The synthesis of V₂O₅ nano-particles involves firstly 0.025 moles of ammonium vanadate was mixed in water (15mL). Resulting solution was added to 60 mL of freshly prepared green tea extract. The reaction mixture was stirred for 3 hours continuously at room temperature. Ammonium hydroxide (10%) solution was added in to reaction mixture in order to maintain pH 10.5. After that reaction mixture was placed for 1 day aging. Then precipitates were separated via centrifugation and washed once with ethanol and twice with deionized water. Sample was heat dried at 80 ⁰C for 16 hours. Calcination of sample was done at 500⁰C for 5 hours, Brick orange colored nano-particles were obtained. Scheme for synthesis of nano-material represented in figure 3.2.

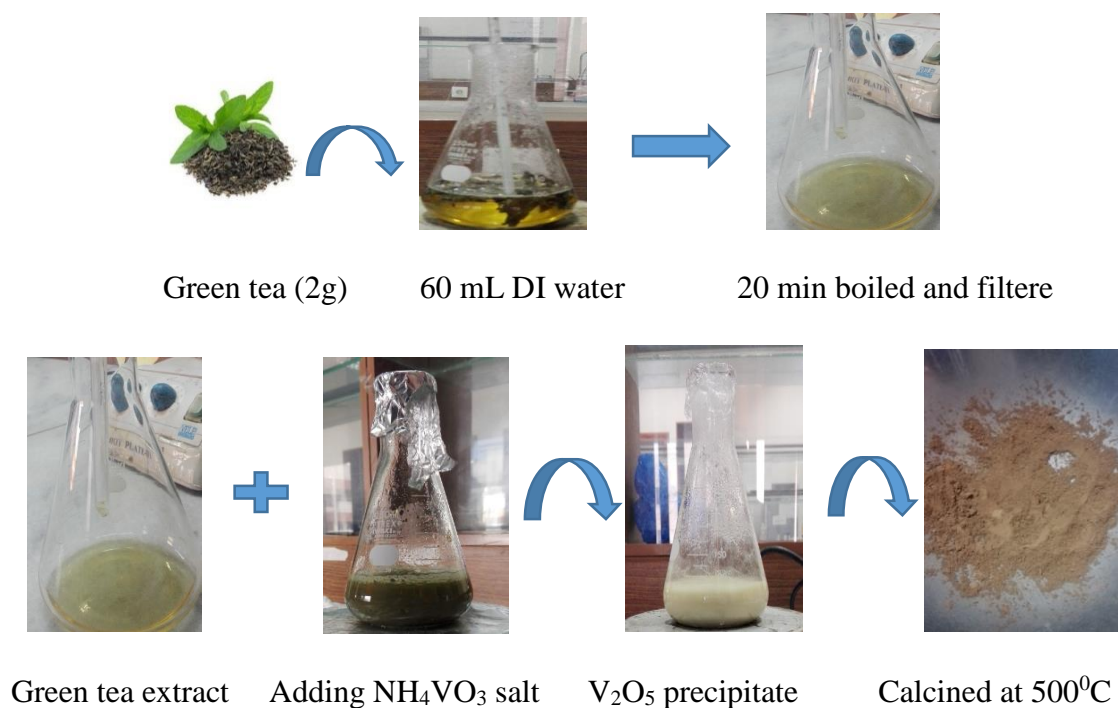


Figure 3. 2 Synthesis of green tea extract and V₂O₅ nano-particles

3.3 Synthesis of polypyrrole:

Polypyrrole was prepared via chemical polymerization in which ferric chloride anhydrous was used as oxidant. 2 g anhydrous ferric chloride was added to 60mL chloroform and was stirred 20 minutes at room temperature i-e 25⁰C . The monomer polypyrrole was distilled to remove inhibitors before using it further. 10 mL distilled pyrrole was drop wise added to ferric chloride solution with constant stirring at 30⁰C. The color of reaction mixture changes to black after adding pyrrole representing generation of polypyrrole. The polypyrrole black precipitates were filtered and washed with methanol and distilled water for removal of ferric chloride and at the end washed with acetone. The black precipitate of polypyrrole was dried at 60⁰C for 8 hours under vaccum. The schematic representation for the synthesis of polypyrrole in being shown in figure 3.3 with conditions being used in prepration.

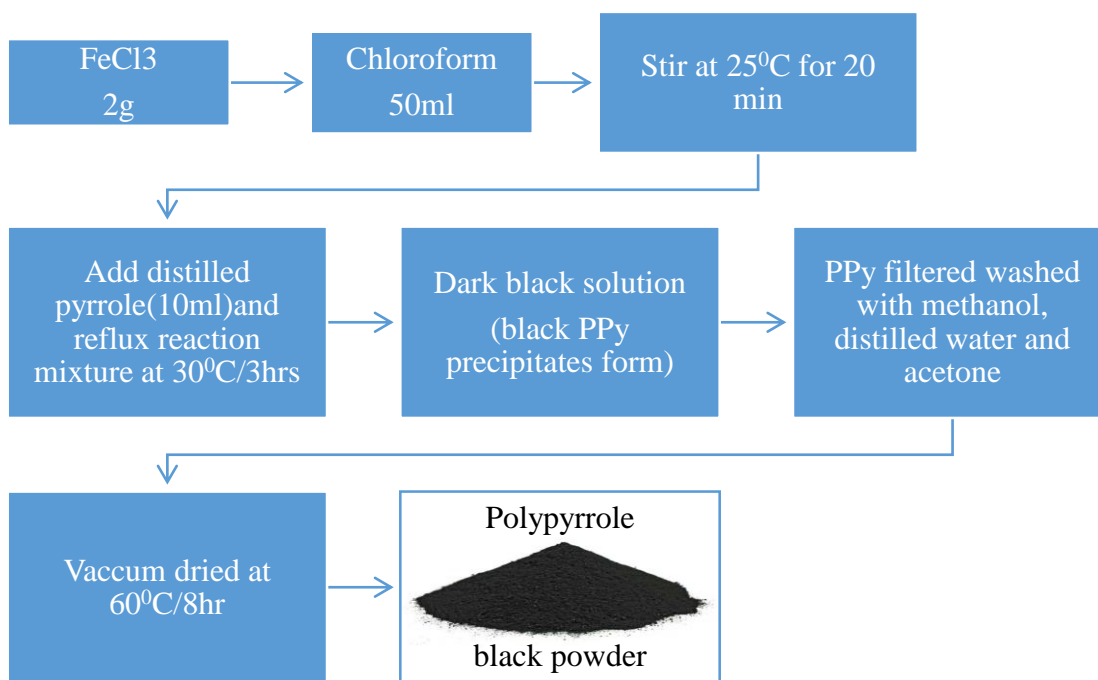


Figure 3. 3 Synthesis scheme of polypyrrole

3.4 Synthesis of PPy/SIS blends:

The synthesis of PPy/SIS blends were done by mixing mechanically SIS copolymer with polypyrrole in varying molar ratios. Chloroform was used as solvent for dispersion of polypyrrole in different weight percent SIS copolymer. The reaction was continuously stirred for 24 hours at room temperature and after thorough dispersal the reaction mixture was spread on Petri dish. It was allowed to dry overnight. Films with 0,2,4,6,8,10,12 and 15 weight percent were made via this process. Films were allowed to dry under vacuum at 60°C for 24 hours. 15 weight percent showed agglomeration of PPy particles with each other. PPy/SIS blends represented in table 3.1:

Amount of SIS	Amount of PPy	PPy/SIS blends
1g SIS	0g PPy	Pure SIS film
0.98g SIS	0.02g PPy	2 Wt% PPy/SIS blend
0.96g SIS	0.04g PPy	4 Wt % PPy/SIS blend
0.94g SIS	0.06g PPy	6 Wt % PPy/SIS blend

Table 3. 1 PPy/SIS blends with different weight percent

3.5 Polymeric nano-composite formation V₂O₅ /PPy-SIS blends:

Nano-composites of V₂O₅/PPy-SIS blends were synthesized by adding nano-particles as reinforcement to PPy/SIS polymer matrix. In this case PPy/SIS acting as matrix phase and nano-particles v₂o₅ act as reinforced phase. The properties of PPy/SIS matrix phase are enhanced by adding v₂o₅ reinforcement. 1-6 weight % composition of V₂O₅ nano-particles was prepared. Nano-particles were dispersed via solution blending method with chloroform as solvent. 24 hours continuous stirring at room temperature was ensured. After uniform dispersal of nano-particles the reaction mixture was poured into petri dish and allowed to dry. 2, 4 and 6 weight% films were prepared and were dried under vacuum at 60°C for 24 hours. Nano-composites are represented in table 3.2:

Amount of SIS	Amount of PPy	Amount of V ₂ O ₅	V ₂ O ₅ /6 wt. % PPy/SIS composite
0.94g SIS	0.06g PPy	0.02g V ₂ O ₅	2 wt.% V ₂ O ₅ /PPy-SIS composite
0.94g SIS	0.06g PPy	0.04g V ₂ O ₅	4 wt. % V ₂ O ₅ /PPy-SIS composite
0.94g SIS	0.06g PPy	0.06g V ₂ O ₅	6 wt.% V ₂ O ₅ /PPy-SIS composite

Table 3. 2 V₂O₅ /PPy-SIS nano-composites with different wt. %

3.6 Characterization techniques:

3.6.1 X-ray Diffractometer:

It is a non-destructive technique used for characterization of phase, size, structure and crystallinity of materials. X-rays are radiations with electromagnetic nature. X-rays show energy within range of 100 eV to 100 KeV. For diffraction x-rays having wavelength 0.1 angstroms are used. This wavelength is equivalent to inter-layer space in crystal lattice. These are called as hard X-rays or short wavelength x-rays. The x-rays show high energy easily penetrates into the material for providing information regarding structure of material i-e structural arrangement. X-ray diffraction follows Bragg's law that explicates monochromatic radiations that are diffracted by crystalline material show constructive interference[90]. These radiations are focused on material or sample via collimator. On interacting with sample material these X-rays results in diffracted rays that on constructive interference can be explained via Bragg's law

$$n\lambda = 2d\sin\theta$$

Here λ is wavelength, n is an integer, d is inter-layer spacing between two planes of crystal whereas θ represent angle of diffraction. Bragg's law is relationship between x-rays wavelength to lattice spacing between planes of crystal and angle of diffraction. X-rays are detected and counted later on. X-ray diffraction from diffraction plan is shown in figure 3.4

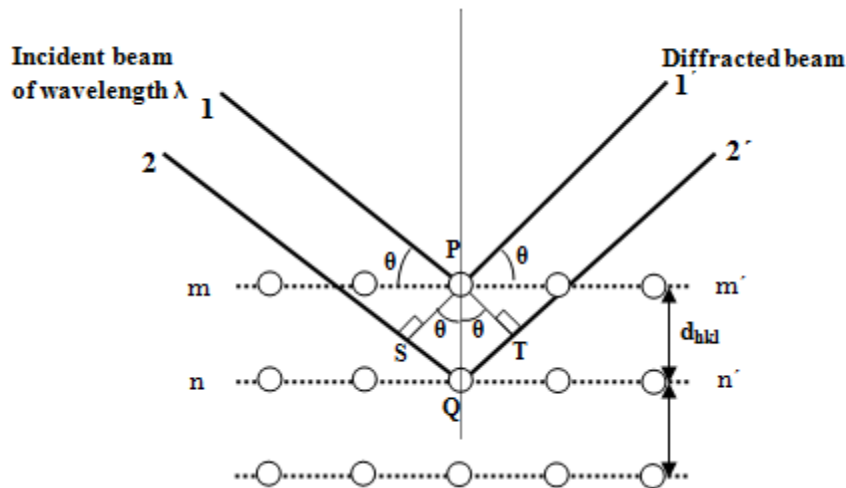


Figure 3. 4 X-rays diffraction from crystal plane

The constituents of X-ray diffractometer includes X-ray tube, sample holder and detector. The X-ray tube contains copper anode that rotates and is source of x-rays. There is negatively charged filament of metal that act as cathode. The generation of X-rays take place by heating negatively charged metal filament present in cathode ray tube to produce electrons. The electrons thus produced are accelerated by applying high voltage in the direction of target. The electrons are bombarded on to the target material i-e anode. If these electrons possess enough energy to penetrate into the target material it will create holes by knocking out inner shell electron. As a result electrons from high energy shell jump to inner shell freeing energy in the form of X-rays forming X-ray spectra. The spectra contain $K\beta$ and $K\alpha$ lines. Usually copper is used as target material in case of single crystal diffraction with $Cu K\alpha$ radiations showing 1.5418 \AA wavelength. $K\alpha$ have $K\alpha_1$ a shorter wavelength and $K\alpha_2$ longer wavelength. Intensity of diffracted X-rays is noted[91].

When Bragg's law is satisfied there will be constructive interference. For detection and processing of X-ray signal charged couple device (CCD) camera detector is used. The signals are converted in to count rate, which is then output into printer[92].

The pattern of XRD obtained are distinctive of material under observation and provide info about:
 (1) shape and size of cell (2) Quantitative analysis can be done using relative peak intensity.

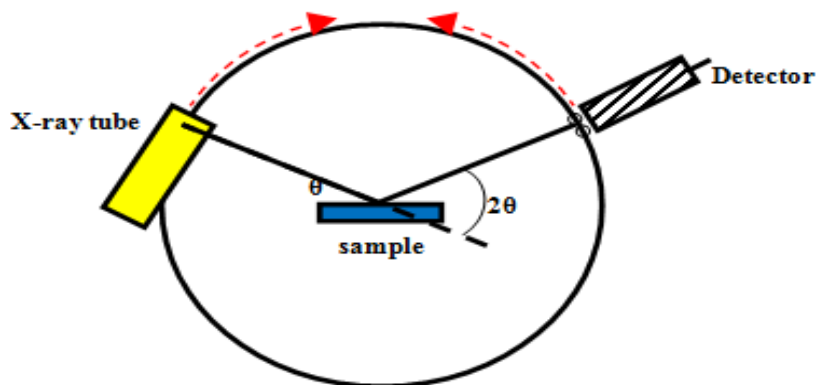


Figure 3.5 Simple X-ray diffractometer

The pattern of XRD obtained are distinctive of material under observation and provide info about:
 (1) shape and size of cell (2) Quantitative analysis can be done using relative peak intensity.

From peak positions unit cell parameters can be calculated by assigning hkl values to each peak i.e indexing. Indexing is prior step for XRD data analysis. It is a complex process. In case of simple structures i.e cubic structure manual indexing can be done but in complicated structures auto-indexing is performed. Following steps involved in indexing: (1) Identification of peak, (2) $\sin^2\theta$ determination, (3) $\sin^2\theta/\sin^2\theta_{\min}$ ratio calculation and multiplication with suitable integer, (4) calculating $h^2+k^2+l^2$ value, (5) Identifying Bravais lattice via comparison of result with $h^2+k^2+l^2$ sequence, (6) calculation of lattice parameters[93]. These steps are represented in table.

Peak No.	2θ	$\sin^2\theta$	$1 \times \frac{\sin^2\theta}{\sin^2\theta_{\min}}$	$2 \times \frac{\sin^2\theta}{\sin^2\theta_{\min}}$	$3 \times \frac{\sin^2\theta}{\sin^2\theta_{\min}}$	$h^2+k^2+l^2$	hkl	a (Å)
1	38.43	0.1083	1.000	2.000	3.000	3	111	4.0538
2	44.67	0.1444	1.333	2.667	4.000	4	200	4.0539
3	65.02	0.2888	2.667	5.333	8.000	8	220	4.0538
4	78.13	0.3972	3.667	7.333	11.000	11	311	4.0538
5	82.33	0.4333	4.000	8.000	12.000	12	222	4.0538
6	98.93	0.5776	5.333	10.665	15.998	16	400	4.0541
7	111.83	0.6859	6.333	12.665	18.998	19	331	4.0540
8	116.36	0.7220	6.666	13.331	19.997	20	420	4.0541

Average lattice parameter is 4.0539 Å

Table 3.3 Indexing of XRD data

Debye-Scherrer's equation is used for calculation of particle size i-e $D = \frac{K\lambda}{\beta \cos\theta}$

Here λ is wavelength of incident X-rays, β is full length at half maxima that is obtained from peak broadening and θ represent Bragg's angle whereas K represent shape factor with value 0.8-0.9. From these values particle size can be calculated[94].

3.6.2 Fourier transform infrared spectroscopy:

The study of vibration of molecule due to absorption of electromagnetic radiation in infrared region i-e 400-4000 cm^{-1} is Fourier transform infrared spectroscopy. The IR spectra breakdown in to two regions:

- < 1000 cm^{-1} called fingerprint region
- 4000-1000 cm^{-1} called functional group region

FTIR provide fingerprint pattern of functional groups hence is used for identification of compounds. Functional groups provide absorption in particular region that is useful for structural analysis of compounds. When IR radiation directed towards sample some of radiations are absorbed by the sample causing change in dipole moment while some are transmitted. Therefore there are various bands in FTIR spectra resultant of in-plane, out-plane, symmetrical and asymmetrical bending[95]. These are shown in figure 3.6 .

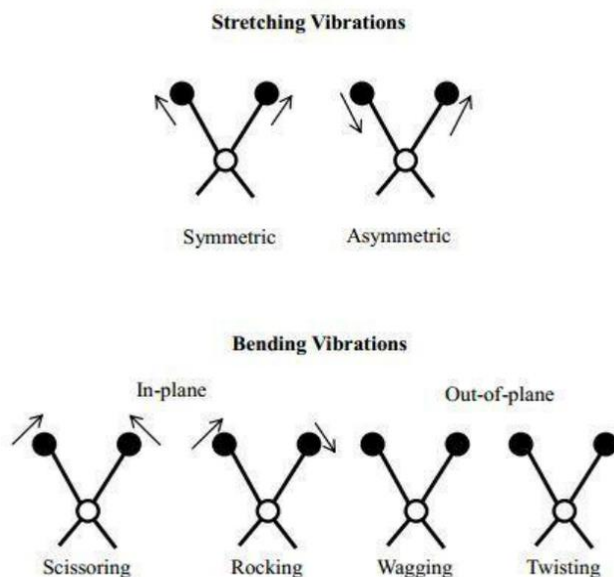


Figure 3. 6: Different types of stretching and bending vibrations

Stretching frequencies are calculated using Hooke's law in which two bonded atoms are taken as simple harmonic oscillator. Hook's law relates frequencies, force constant and atomic masses of two bonded atoms[96]. Hook's law equation is given as:

$$\text{Stretching frequency} = \bar{\nu} = \frac{1}{2\pi c} \left[f \frac{m_A + m_B}{m_A m_B} \right]^{1/2}$$

Here c is velocity of light in cm/s , ν is vibration frequency in cm^{-1} , m_A or m_B are masses for atom A and B respectively and f is force constant of bond in dyne/cm . In FTIR following components are present i-e source, sample holder, monochromator and detector. IR radiations are generated at source and then allowed to pass through wavelength selector called monochromator after that move to interferometer here spectral encoding is done. After that beam of single wavelength move through sample in which some radiations are with specific frequency are absorbed while others

are transmitted. These are detected via detector that is specifically designed to measure particular interferogram signals. The signal undergoes Fourier transformation via computer producing spectra with bands as function of wave number[97].

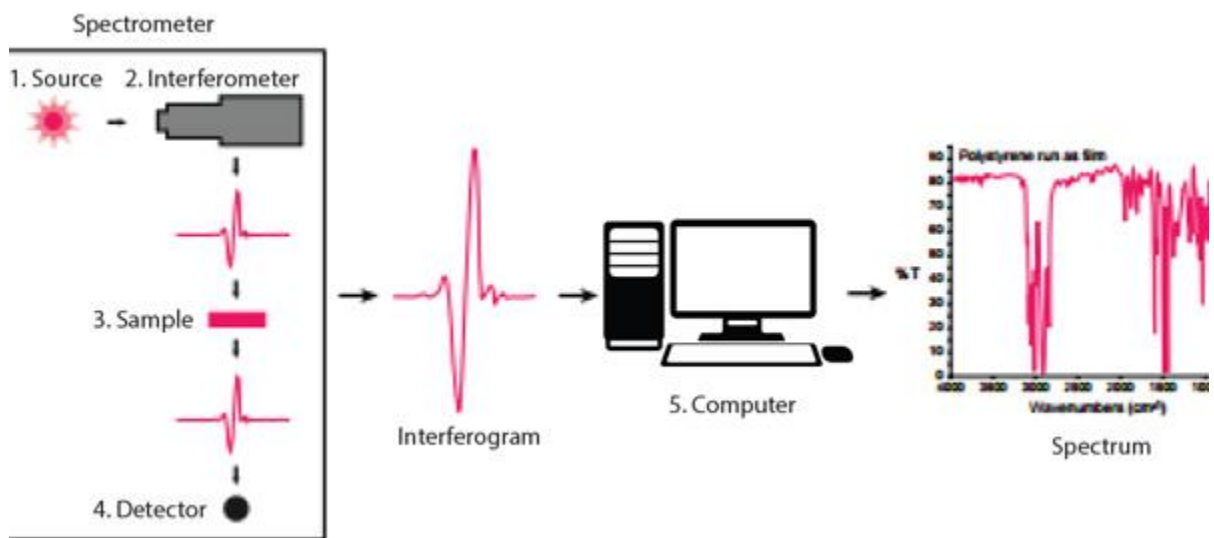


Figure 3.7 Fourier transform infrared spectroscopy

3.6.3 Scanning electron microscopy coupled with EDX

SEM is an imaging system that provides information about surface morphology by concentrating beam of electron having high energy over sample. Beam of electron provides improved resolution comparative to optical light and produce range of signals during interaction with specimen. For traditional SEM system about 1 cm to 5 microns in width can be sketched. In SEM electrons having high energy are accelerated towards target. When high energy electron are interacted with specimen energy is released in form of secondary electrons, diffracted back scattered electrons, back scattered electrons, heat, visible light and photon. The signals are treated via detector that generate sketch of specimen on cathode ray screen. BSE and SE provide information relating contrast with composition and topography respectively[98].

The components of scanning electron microscopy includes electron column and electron console. Electron console is made up of switches to regulate filament voltage, current, contrast, brightness

and magnification. Electron beam produced under vacuum in electron column and concentrated on certain area of sample via electromagnetic scanning coil. Lower part of column is specimen chamber[99]. Within specimen chamber above sample stage a detector for secondary electron is present. Sample stage is controlled via goniometer. Electron column made up of following parts: aperture, electronic gun, condenser lenses, specimen chamber and scanning system. At the top of electron column electron gun is present. In an electron column beam of electron is produced via tungsten filament when heated at approximately 2700K. These electrons are accelerated to anode via 200V to 3 KV. Electron beam is converged via two condenser lens after passing through anode. Apertures in electron column shorten and reject inessential electrons in lenses. Spot size of beam at sample or specimen is determined by final lens aperture[100]. The decrease in spot size will result in increase of depth of field and resolution. Stigmator located at end of objective lens used to decrease deviation of electron beam. At lower portion of column specimen chamber is located. Secondary electron signals coming out of sample or specimen are focused on to detector via positive charge. SEM work under high vacuum as 2700K temperature of filament can be easily reached in vacuum conditions, column optics work efficiently in dust free condition and electron beams can reach specimen without any interruption[101].

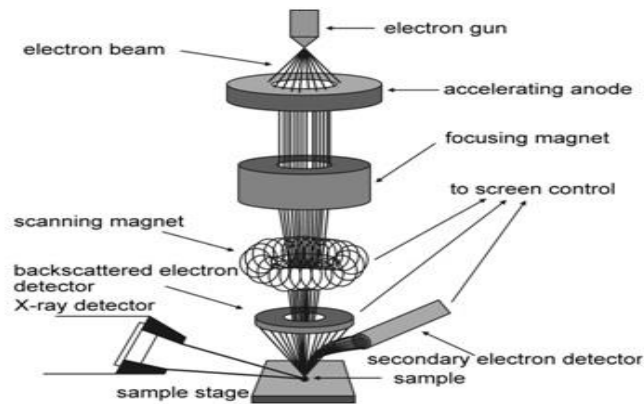


Figure 3. 8: Schematic of scanning electron microscopy

The variety of signals are generated when beam of electron strikes with sample or specimen shown in figure. Two types of signals are involved in providing information about visuals and surface morphology. These signals are from backscattered and secondary electrons. Inelastic collision with specimen generate secondary electrons and possess energy < 50 eV providing information about surface of sample. Elastic collision with atom nuclei of sample create backscattered electrons. These electrons enter

deep in to the sample to provide atomic number contrast and topographical contrast. Back scattered electron detector is used to detect density variations. On interaction with sample X-ray signals can also be generated providing information about surface composition[102].

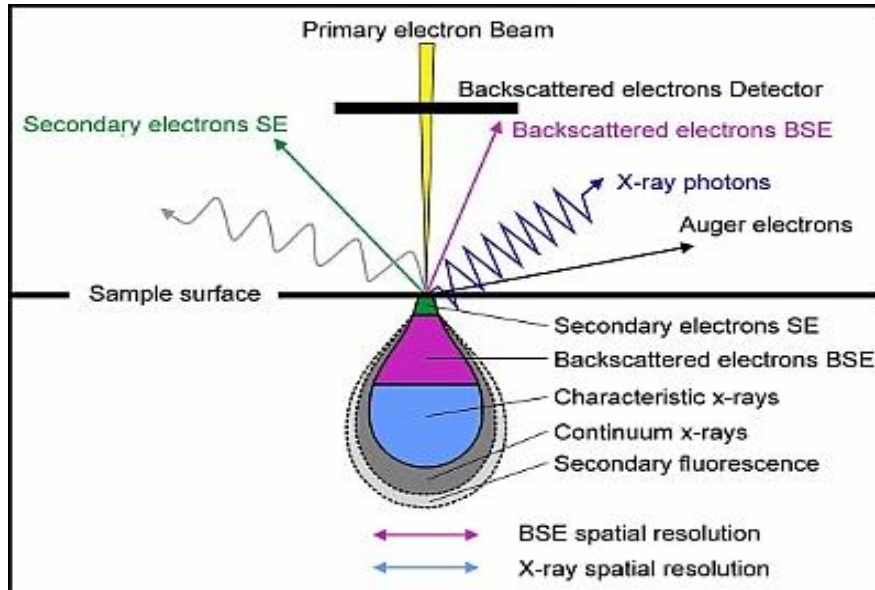


Figure 3. 9: Different signals generated by specimen-electron beam interaction

Scanning electron microscopy (SEM) and transmission electron microscopy (TEM) are coupled with EDX systems. Energy dispersive X-ray spectroscopy is helpful for elemental analysis of specimen using X-ray spectra radiated by solid sample. It includes interaction of specimen and electron beam producing various signals having specific X-rays of various elements. The characteristic X-rays are separated via energy dispersive detector that is analysed using EDX system software to conclude abundance of particular element. EDX is used to generate elemental map. It is used to detect elements from Be_4 to U_{92} . EDX detector is sensitive to X-rays[103]. It work in nitrogen atmosphere and there is a software used to analyze spectrum. Detector is fitted at the end of long arm equipped with nitrogen cooling system with in the sample chamber. Highly sensitive detectors mostly operate at low voltage and are made up of Si(Li) crystal. Most recent silicon drift detector showing high count rate and these work without any nitrogen cooling system.

Energy of these electrons get absorbed by crystal present in EDX detector via ionization. Resulting free electrons inside crystal, it become conductive and generating an electric charge bias. X-ray absorption converts separate specific X-rays to electric signals. EDX data is collected as energy peaks relating to respective element in specimen and spectra attained between energy in KeV and X-ray count, providing composition of specimen under observation. Usually energy peaks are narrow and multiple peaks are generated in case of many elements. Low intensity peaks show low abundance of elements and their resolution is not easy. EDX is a non-destructive technique and is performed with little or no sample processing[103].

3.6.4 Mechanical testing:

Tensile strength is a measure of stress a material can bear before breaking. It is measured via a mechanical testing machine. The basic principle is applying continuous increasing strain up to fracture of specimen, to conclude tensile strength, percentage elongation and ductility of material by percentage reduction of area[104].

ASTM standards are used for mechanical testing i.e. resistance of material against applied force. Mechanical tests provide information about stiffness, ductility and strength of material. The sample or specimen is fixed in a tensile testing machine in a precise way and deformed via force[105]. The machine consists of a moveable grip or wedge moving with fixed velocity to elongate sample up to fracture point and a static grip. Strain gauge is used to measure elongation of specimen. Force vs displacement curve is used to show output and then converted to stress vs percentage strain curve. Schematic representation is shown in figure. Various tensile properties such as stress at fracture point, Young's modulus, percentage elongation and percentage strain at fracture point etc can be determined via stress vs percentage strain curve. Tensile strength of materials in form of thin films with < 1 mm thickness can be measured using ASTM D882 standard.

According to ASTM D882 gauge length is selected before start of test i.e. for polymer film is 20 mm. Cross sectional area is determined from thickness and width of specimen for every sample that is 0.34 mm and 10 mm respectively. The specimen is then mounted on to the machine and remote connection is built up.

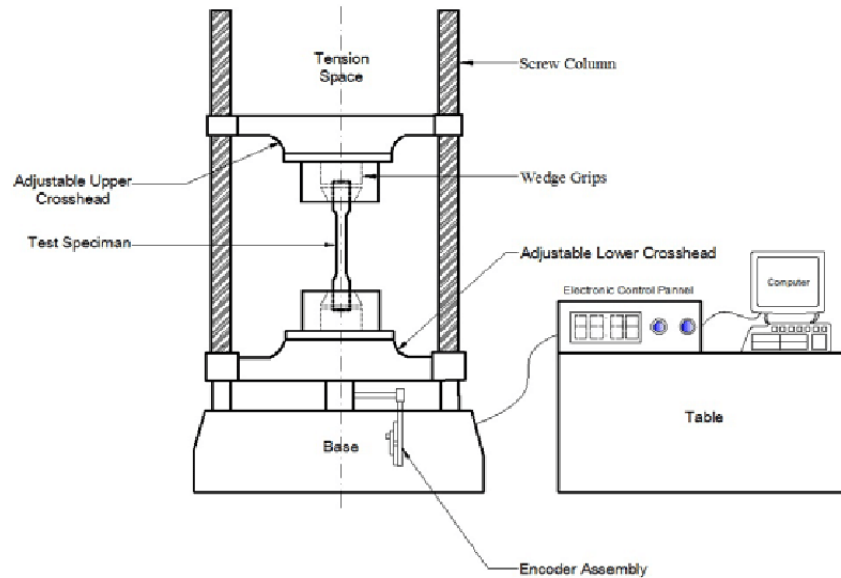


Figure 3. 10 Schematic representation of tensile testing machine

One end of sample or specimen is fitted in static grip and other end is moved continuously via fixed velocity until specimen break. On developing remote connection live images are shown on computer following already set test parameters, starting test and the data is saved. The test continue upto breakage of sample. The results are shown in graph of force vs displacement that is converted to stress vs percentage strain curve[106]. Force applied per unit area to create deformation in sample is known as stress. Ratio of load applied to original area of cross-section is know as stress.

$$\sigma = F / W \times d$$

Ratio of change in length to original length of sample is known as strain. It is a dimensionless ratio.

$$\text{Strain} = \text{Change in length} / \text{original length of specimen}$$

$$\varepsilon = \Delta L / L$$

Dimensions of tensile test specimen is represented in table:

Symbol, definition	Dimensions of specimens (mm)
W, width of narrow section	10
T, thickness of specimen	0.34
D, distance between grips	20
L, total length of specimen	40

Table 3.4 Tensile test specimen dimensions

Young's modulus: It is ratio of stress to strain below proportional limit of specimen, determined by sketching tangent to first point of deformation and calculating slope between stress-strain curves.

$$\text{Young's modulus} = \frac{\text{stress}}{\text{strain}}$$

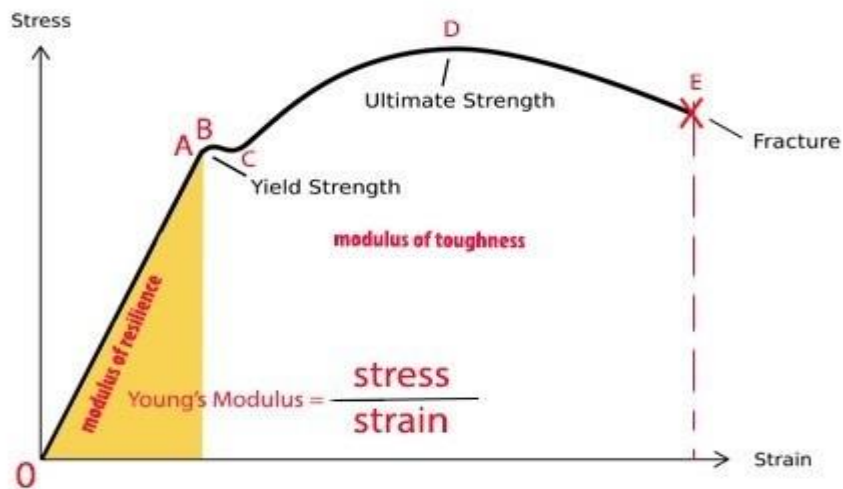


Figure 3. 11 Young's modulus determination

Proportional Limit: The point where stress and strain remains proportional is called as proportional limit point.

Elastic Limit: The limit to which material remain elastic is elastic limit.

Ultimate stress point: The highest stress film can bear before breaking is known as ultimate stress point.

Breaking Stress: The point where strength of material break down is known as breaking stress.

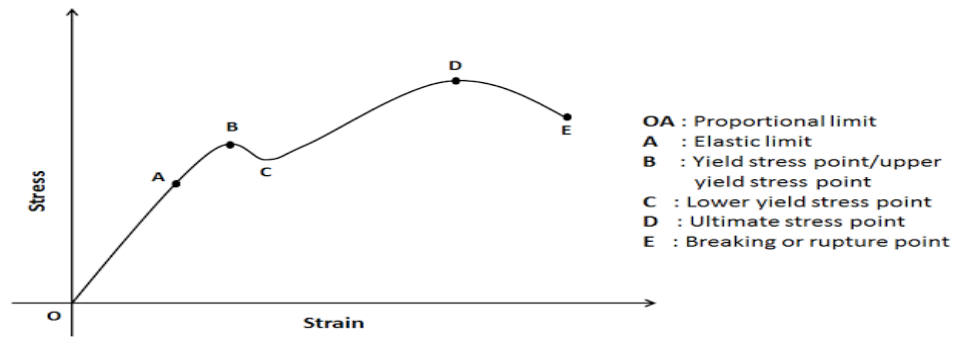


Figure 3. 11 Stress-Strain curve

Calculating strength of material via stress-strain curve:

Area under stress-strain curve provide stress of specimen. Brittle specimen show less strain and high stress. The area under stress-strain curve decrease with increase of strength of specimen. An elastic specimen has high stress and low strain. In this case increase of area under curve occur. Specimen A is brittle comparative to B and C whereas D is highly flexible specimen showing high strain and low stress[106].

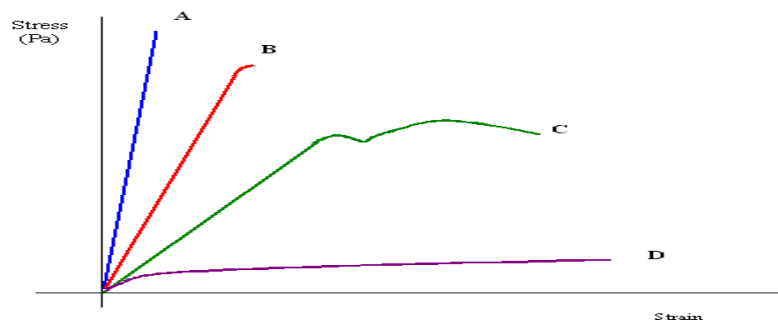


Figure 3. 12: Reduction in area under curve with increase in strength

3.6.5 Two point probe conductivity measurement:

One of important property of material is electrical conductivity. There are two most favourite techniques used to determine electrical conductivity. One is Two point probe conductivity measurement while second is four point probe process. Two point probe technique is used for material showing high resistance whereas four point technique is used for low resistance material. Two point probe is less expensive and simple technique comparative to four point probe technique.

Ohm's law is used to measure electrical conductivity that relates applied voltage and current flow through conductor. It is defined as: The potential difference is directly proportional to current flowing through conductor. Ohm's law is represented by:

$$V \propto I$$

$$V = IR \text{ or } R = V/I$$

Here I is current flow, V is potential difference and R represent resistance. Inverse of resistance is conductance. Its unit is Siemens. It is represented by following equation:

$$C = 1/R$$

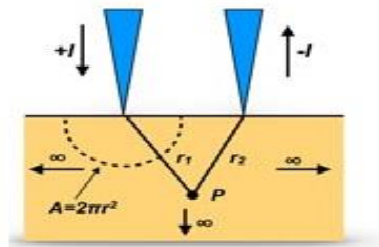


Figure 3. 13: Two point probe conductivity measurement

Alternating current applied between two point tip and potential difference across two point in order to determine resistance of sample according to two point probe technique. This technique contains conductometer that is made up of osmium or tungsten carbide probe tips. These probe tips are hanged at end of separate arm. The motion of probe tip is controlled by pivots on kinematics bearing when come interact with specimen. Two probes tips are parted at 20 μm distance. Two probe tips lowered to the specimen to calculate resistance. Electrodes are supported on specimen

by applying silver conducting paste on the specimen surface, for determining electrical resistivity of specimen. Resistivity of specimen is determined via equation:

$$\rho_s = \frac{V \times A}{I \times t} = \frac{R_s \times A}{t}$$

Here A is cross-sectional area of specimen, R_s is surface resistivity of specimen and t represent distance between two probe electrodes on specimen. The inverse of resistivity is conductivity hence from resistivity, conductivity value can be measured.

$$\sigma = 1/\rho$$

Here ρ is resistivity and σ represent conductivity of specimen. Unit for resistivity is Ohm meter ($\Omega.m$)

Chapter 4

Results and discussion

4.1 Synthesis and characterization of V_2O_5 nano-particles:

4.1.1 Synthesis of V_2O_5 nano-particles:

V_2O_5 nano-particles was synthesized via green synthesis using green tea extract that act as reducing agent. Green tea leave extract composed of rich concentration of polyphenols catechins, proteins, vitamins and carbohydrates. They act as capping agent as well as reducing agent. The synthesis of V_2O_5 nano-particles involves firstly 0.025 moles of ammonium vanadate was mixed in water (15mL). Resulting solution was added to 60 mL of freshly prepared green tea extract. The reaction mixture was stirred for 3 hours continuously at room temperature. Ammonium hydroxide (10%) solution was added in to reaction mixture in order to maintain pH 10.5. After that reaction mixture was placed for 1 day aging. Then precipitates were separated via centrifugation and washed once with ethanol and twice with deionized water. Sample was heat dried at 80 °C for 16 hours. Calcination of sample was done at 500°C for 5 hours, Brick orange colored V_2O_5 nano-particles were obtained. Formation of nanoparticles was confirmed by XRD, SEM and FTIR analysis.

4.1.2 X-ray diffraction analysis of V₂O₅ nano-particles

The synthesis of V₂O₅ nano-particles and crystalline structure was confirmed using X-ray analysis. X-ray diffractometer used CuK α as source of radiation having (0.154nm) wavelength. It has monochromator made of graphite with 2θ in (5°-80°) range. Analysis performed at room temperature.

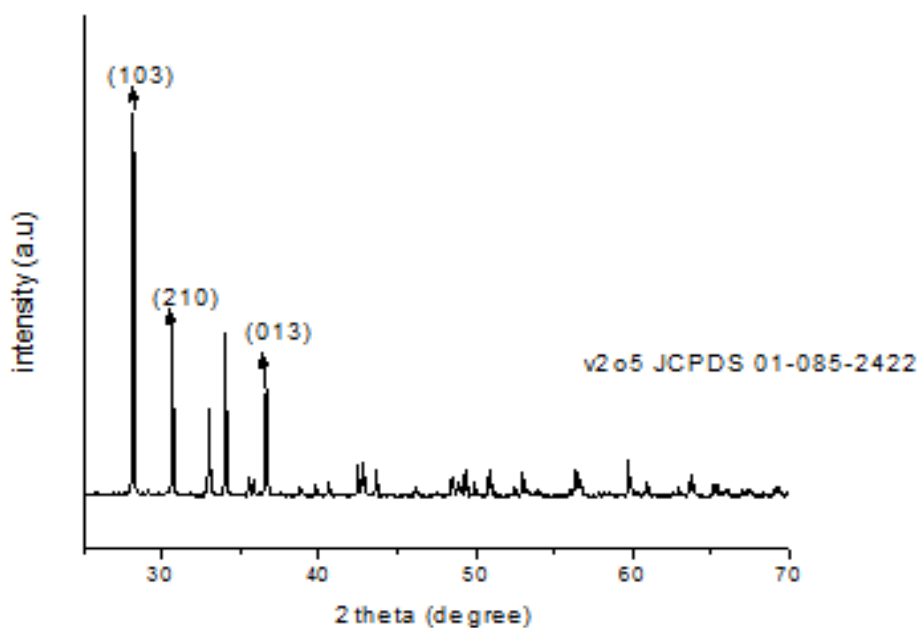


Figure 4.1 XRD of V₂O₅ nano-particles

The hkl values matched quiet well with the reference that confirmed formation of crystallites [107]. The average size of particles calculated to be 40.2nm.

4.1.3 FT-IR analysis for V₂O₅ nano-particles:

To ratify capping and reducing agent from green tea extract i-e polyphenolic content and interaction if these biomolecules with V₂O₅ nano-particles their FT-IR analysis was done via spectrophotometer in 4000-500 cm⁻¹ range.

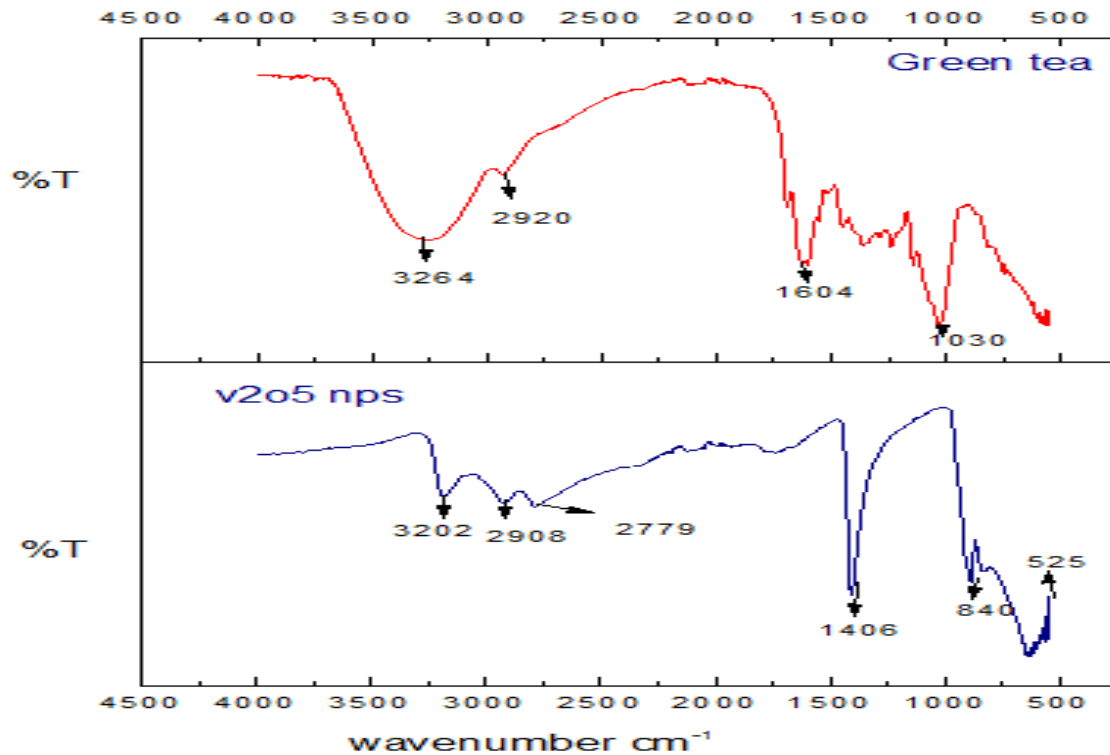


Figure 4. 2: FT-IR of V_2O_5 nano-particles and Green tea extract

The IR spectrum for V_2O_5 nano-particles showed characteristic metal-oxygen-metal bands at 525cm^{-1} and 840 cm^{-1} [108]. At 3264 cm^{-1} $-OH$ stretching vibration is for phenolic content or biomolecules and at 2779 cm^{-1} $O-H$ stretch is for carboxylic acid [109]. At 1406 cm^{-1} $C=C$ vibration for alkanes and 2920 cm^{-1} is for $C-H$ stretch in alkane. The phenolic content was confirmed helped in reduction and carboxylic content helped in stability of nano-particles.

4.1.4 Energy dispersive X-ray spectroscopy:

The synthesis of V_2O_5 nano-particles was confirmed via EDS analysis. The composition of element of V_2O_5 was found out from EDS data represented in figure below:

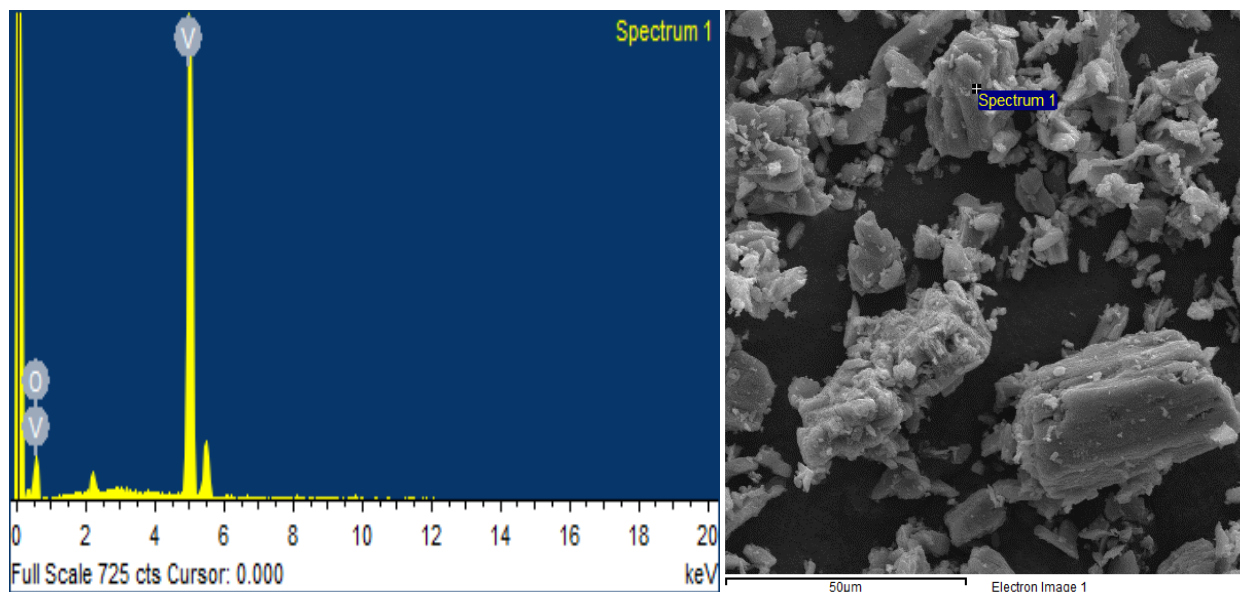


Figure 4.3 : EDS for V_2O_5 nano-particles

Presence of V and O is confirmed from the spectrum.

4.2 Formation and characterization of polypyrrole:

The preparation of polypyrrole black precipitates was done and its formation was confirmed via FT-IR analysis and XRD.

4.2.1 Synthesis of polypyrrole:

Polypyrrole was prepared via chemical polymerization in which ferric chloride anhydrous was used as oxidant. 2 g anhydrous ferric chloride was added to 60mL chloroform and was stirred 20 minutes at room temperature i-e $25^{\circ}C$. The monomer polypyrrole was distilled to remove inhibitors before using it further. 10 mL distilled pyrrole was drop wise added to ferric chloride solution with constant stirring at $30^{\circ}C$. The color of reaction mixture changes to black after adding pyrrole representing generation of polypyrrole. The polypyrrole black precipitates were filtered and washed with methanol and distilled water for removal of ferric chloride and at the end washed with acetone. The black precipitate of polypyrrole was dried at $60^{\circ}C$ for 8 hours under vacuum. It was prepared in the form of black coloured precipitates and synthesis was characterized via XRD and FT-IR characterization.

4.2.2 X-ray Diffractometer:

The synthesis of polypyrrole and crystalline structure was confirmed using X-ray analysis. X-ray diffractometer used $\text{CuK}\alpha$ as source of radiation having (0.154nm) wavelength. It has monochromator made of graphite with 2θ in (5° - 80°) range. Analysis performed at room temperature.

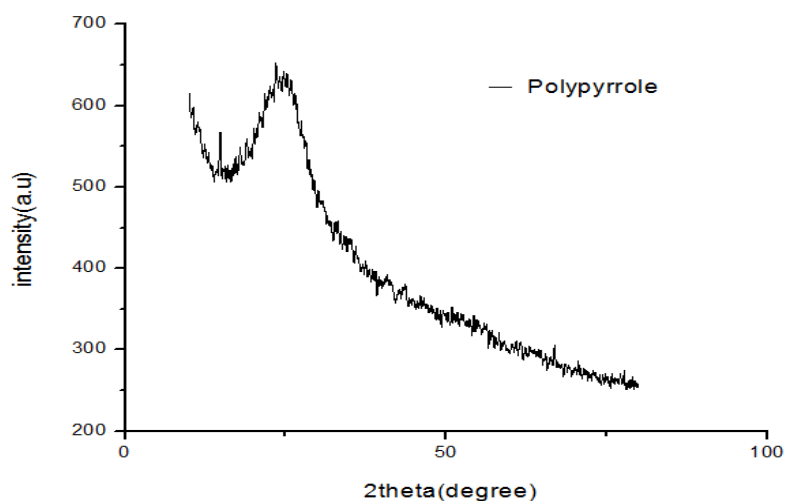


Figure 4. 4: XRD pattern of polypyrrole

The XRD pattern for polypyrrole coordinated well with reference [110]. Highest intensity peak's chain separation calculated via formula:

$$S = \frac{5\lambda}{8\sin\theta}$$

Here S represent chain separation, X-ray wavelength denoted by λ and θ is angle of high intensity peak and for peak 23.6° chain separation figured out to be 4.8 \AA .

4.2.3 FT-IR analysis of polypyrrole:

To ratify polypyrrole synthesis FT-IR analysis of sample was done via spectrophotometer in 4000 - 500 cm^{-1} range. FT-IR spectrum for polypyrrole showed certain characteristic bands in following region as represented in figure:

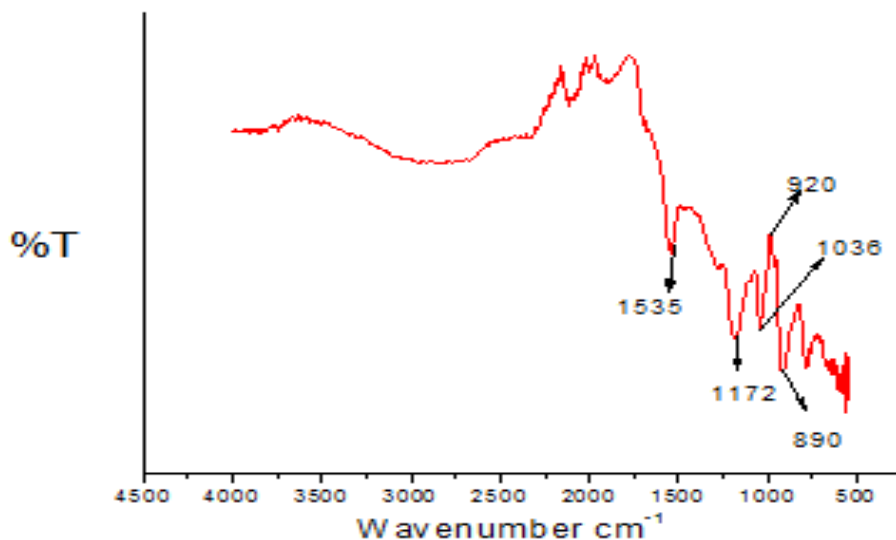


Figure 4.5 FT-IR of Polypyrrole

The band at 1535cm^{-1} is characteristic C=C vibration for pyrrole ring and at 1400 cm^{-1} is C=N stretching vibration for pyrrole ring. There is C-N bending stretch at 1172 cm^{-1} and 920 cm^{-1} band is for C-H wagging vibration. The bands at 890 cm^{-1} and 1036 cm^{-1} represents out of plane vibration =C-H bond and in plane vibration of =C-H bond respectively[111]. These results of FT-IR confirmed polypyrrole synthesis.

4.3 Formation and characterization of Poly SIS/PPY blends:

4.3.1 Synthesis of Poly SIS/PPY blends:

Poly SIS/PPY blends was prepared via solution blending method in which polypyrrole mixed with poly SIS via continuous stirring at room temperature for 24 hours using chloroform as solvent media and the films was oven dried for 8 hours at 70°C placed in glass petri dish. Different weight percent composition from 0-8 wt. % was prepared. Their formation was confirmed via FT-IR. The figure 4.6 represents the comparison FT-IR of blend of poly SIS/PPY and pure SIS showing shift in peak intensities and change of few peaks representing the mixing or blending of two polymers hence confirming blend formation. The higher concentration of PPY did not formed the films properly due to poor interaction between two polymers at increased concentration.

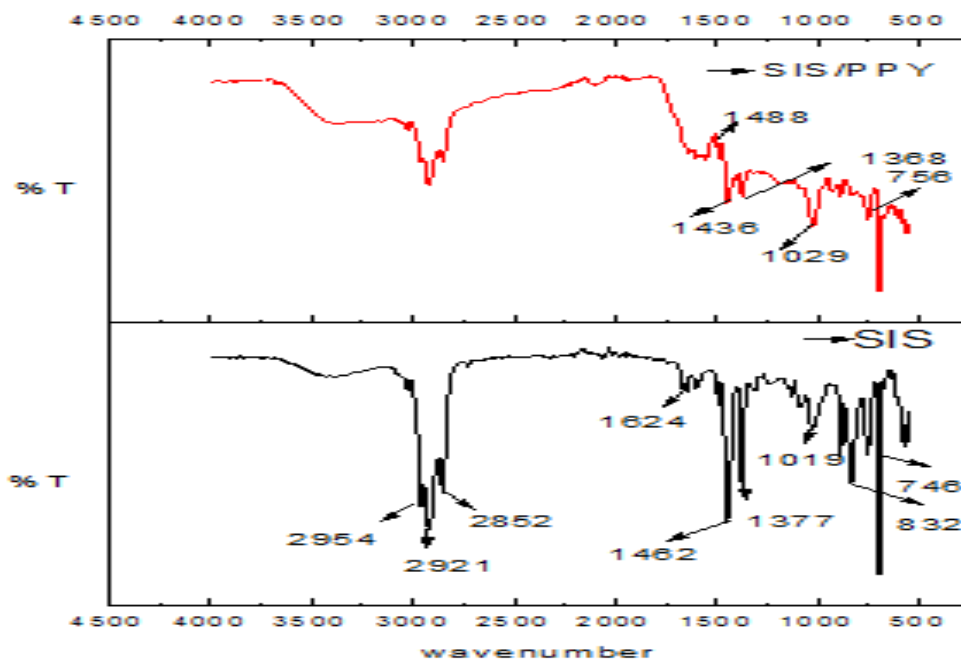


Figure 4. 5: FT-IR of Poly SIS/PPY blend and SIS polymer

FT-IR analysis was performed via BRUKER spectrophotometer from 4000-500 cm^{-1} wavelength range. The bands at 2952 cm^{-1} and 2921 cm^{-1} represents symmetric and asymmetric vibration of aromatic ring respectively. The 2862 cm^{-1} is C-H aliphatic chain stretch and 1624 cm^{-1} is aromatic ring C=C stretch. The 1402 cm^{-1} is C-H bending of aliphatic chain. A new band at 1029 cm^{-1} represent N-H bond deformation shown in figure 4.6. The physical mixing of two polymers confirmed by change in peak intensities, position of peaks and formation of new peaks. The comparison of pure poly SIS and the blend of poly SIS/PPY is being shown via figure that represent clear changes in two FT-IR peaks showing the physical interactions of two polymers.

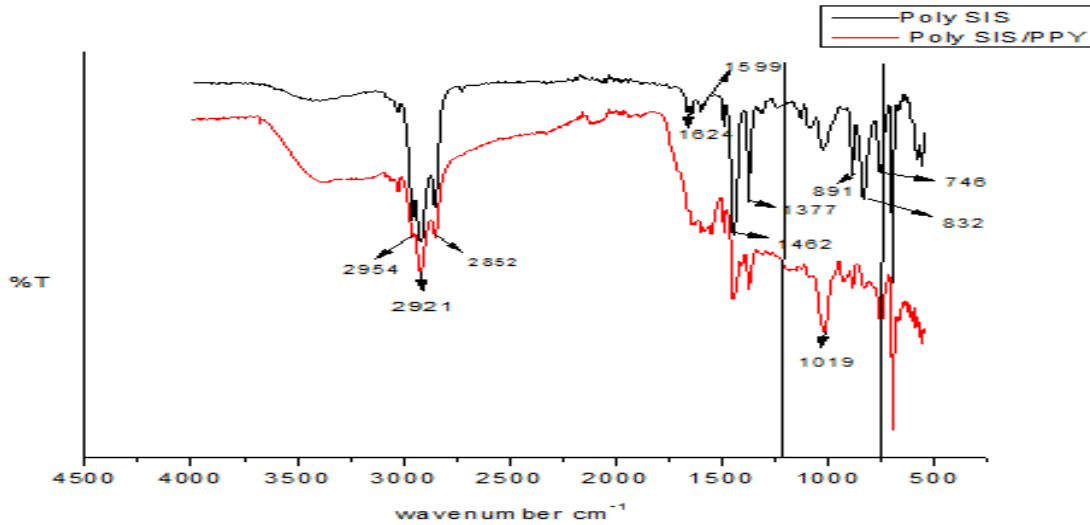


Figure 4. 6: FT-IR comparison of poly SIS/PPY and pure SIS

4.4 Formation and characterization of Poly SIS/PPY- V_2O_5 polymeric nano-composites:

4.4.1 Formation of polymeric nano-composites:

Polymeric nano-composite was synthesized by using V_2O_5 nano-particles as reinforcement phase poly SIS/PPY being matrix phase. Nano-particles were added in different concentration from 0-8 wt. %.

4.4.2 Mechanical testing of Poly SIS/PPY- V_2O_5 Composites:

Tensile test was done for different weight percent composition of blends as well as pure poly SIS in order to observe the change in mechanical properties of blends and pure polymer. ASTM D882 standards was followed for polymer. The area of stress-strain curve is the energy needed to break sample material. The response of PPY on tensile strength, Young's modulus and % strain at the breakage point was observed and represented in figure 4.8 below for each different weight percent blend of Poly SIS/PPY i-e pure SIS (a), 6% blend (b), 4% blend (c), 2% blend (d) :

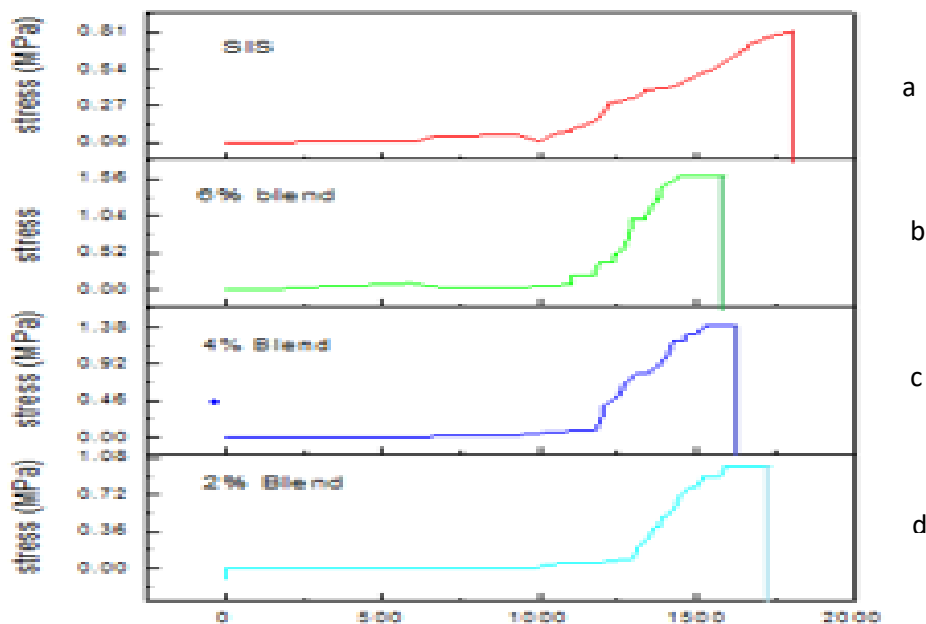


Figure 4. 7 Stress vs. % strain curve for (a) 0 %, (b) 6%, (c) 4%, (d) 2% blend

For pure poly SIS %strain at breakage was 1799 % and tensile strength observed at 0.81MPa curve a ; whereas Young’s modulus found to be 0.045. The change in mechanical behavior of blends due to addition of PPY in poly SIS can be clearly understood via the stress vs % strain curve of pure SIS and Poly SIS/PPY with different weight % bends. For 2% blend % strain at breakage observed at 1740 % whereas tensile strength was at 1 MPa curve b and Young’s modulus calculated as 0.057. PPY is brittle in nature with the addition of PPY into poly SIS there is decrease in area under stress – %strain curve that means now lesser energy needed for breakage of film. Increase in stress with decrease in % strain at breakage was observed.

Further addition of PPY to poly SIS i-e 4 % concentration there is further increase of tensile strength to 1.4 MPa with decrease of % strain at breakage i-e 1633 % curve c and young’s modulus calculated as 0.085.

There is gradual increase in tensile strength and young’s modulus showing increase in strength of films with decrease in area under stress- % strain representing lesser amount of energy needed for breakage of films.

Curve d 6 % addition of PPY to poly SIS results in tensile strength of 1.6 MPa and % strain at break as 1600 % whereas Young's modulus calculated 0.1. The reason for this change is that when PPY is added to Poly SIS there is disturbance in the polymeric matrix and the weak interaction occur between poly SIS and PPY that results in decreasing flexibility of co-polymer.

PPY content wt. %	YOUNG'S Modulus MPa	Tensile strength MPa	%strain at breakage
0%	0.045	0.81	1799
2%	0.057	1	1740
4%	0.085	1.4	1633
6%	0.1	1.6	1600

Table 4. 1 Young's modulus for 0%, 2%, 4%, 6% Poly SIS/PPY blends

According to above data 6 % poly SIS/PPY blend show best results regarding mechanical properties. In order to study the result of addition of nano-particles as reinforcement phase 6 % poly SIS/PPY blend is being used in which nano-particles from 2-6 % was added. The same mechanical test was done with the composites prepared by adding different weight % of nano-particles in to the poly SIS/PPY blends forming poly SIS/PPY-V₂O₅ blends. Results represented in the figure 4.9. The stress vs % strain graph for each % composite of Poly SIS/PPY-V₂O₅ is being represented via a comparison graph in which 6% composite Poly SIS/PPY-V₂O₅ is shown as (a) , 4% composite represented as (b) while 2% composites represented as (c). Graph data was obtained from tensile testing. While testing different % composites 5mm/min rate was used to obtain desired results. The samples with higher concentration of nano-particles were also tested that resulted in non-uniform films which could not be used for mechanical testing. From comparison graph it can be seen that with increasing concentration of nano-particles tensile strength keep on increasing and area under cover decreases gradually showing less amount of energy required to break each sample.

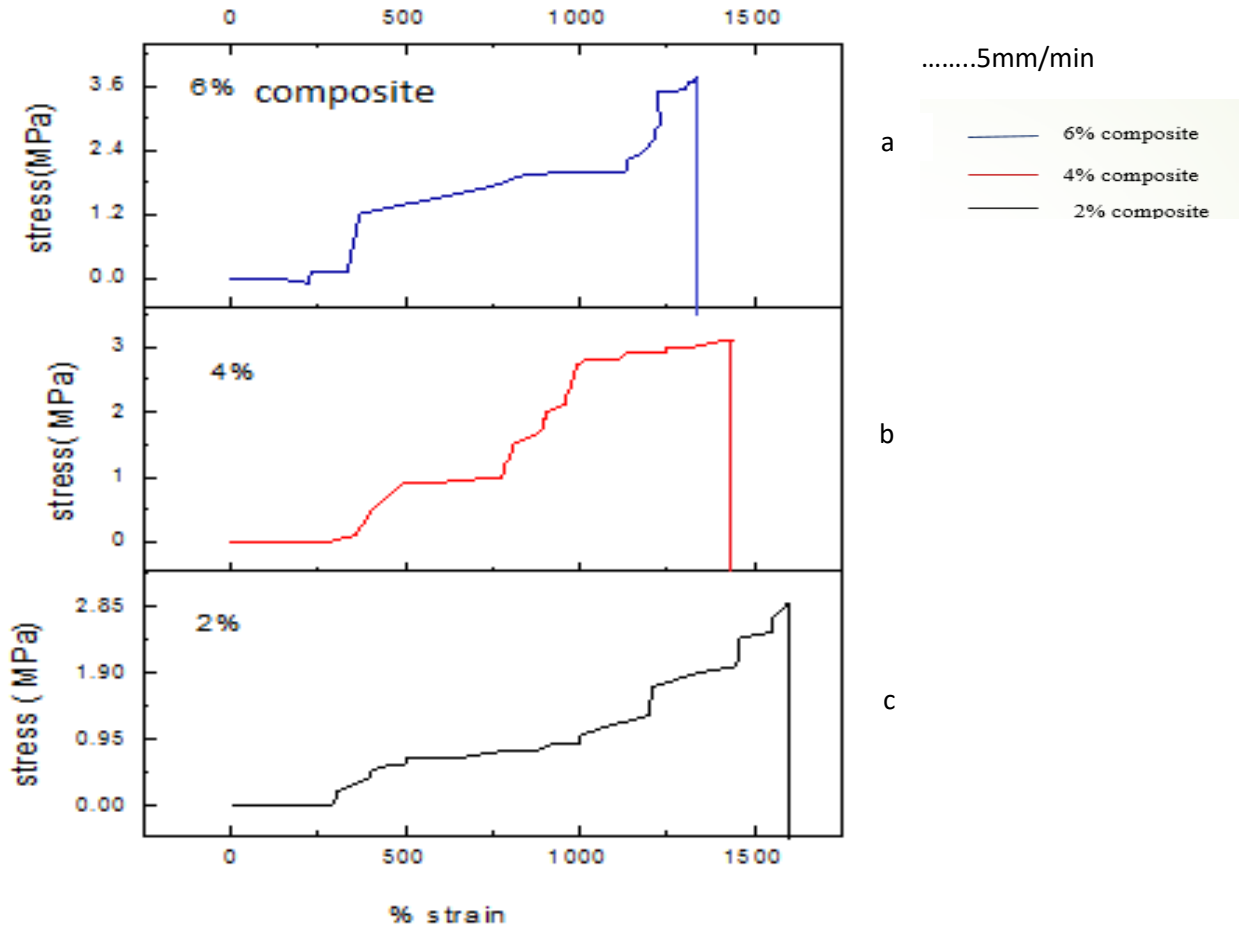


Figure 4. 8 Stress vs % strain curve for composites (a) 6% V_2O_5 composite (b) 4% V_2O_5 composite (c) 2% V_2O_5 composite

The incorporation of V_2O_5 nano-particle to poly SIS/PPY blends changes the mechanical behavior of films that can be clearly seen in the figure above. Adding just 2 wt. % of nano-particles dramatically increase tensile strength of films i-e 2.9MPa and % strain at breakage decrease to 1595 %. The area under stress-strain curve decrease representing lesser amount of energy is needed to break film but increase in Young's modulus show increase in strength of polymeric nano-composite films.

With further addition of 4% nano-particles stress increase to 3.1 MPa and % strain decrease to 1443 % curve b and Young's modulus calculated to be 0.21. With 6% addition of nano-particles tensile strength increases to 3.8 MPa and % strain at 1333% curve c and Young's modulus calculated as 0.28. The addition of nano-particles to the polymeric blends decrease elongation of

poly SIS but increase in strength and stiffness of the films. Nano-particles because of their size show excellent effects on mechanical properties of composites as composites show good mechanical strength as compare to the polymeric blends.

V ₂ O ₅ content wt. %	YOUNG'S Modulus MPa	Tensile strength MPa	%strain at breakage
2%	0.18	2.9	1595
4%	0.21	3.1	1443
6%	0.28	3.8	1333

Table 4. 2 Young's modulus for 2%, 4%, 6% poly SIS/PPY-V₂O₅ Composites

4.5 Conclusions:

In present research work V₂O₅ nano-particles were prepared using green chemistry method that is using green tea extract. The synthesis was confirmed using XRD and FT-IR characterization techniques. From XRD average crystallite size calculated 39.8nm. FT-IR spectra confirmed characteristic bands for nano-particles synthesis. Elemental composition was confirmed by EDS analysis that confirmed presence of vanadium and oxygen. The synthesis of polypyrrole was done via chemical polymerization method. Its synthesis was confirmed via XRD where chain separation for high intensity peak 23.6° calculated 4.8Å. FT-IR spectra showed 1535 and 1400 cm⁻¹ characteristic peaks confirming synthesis of polypyrrole. Poly SIS/PPY blends with different wt. % of PPY was formed that increased film forming properties of PPY. FT-IR spectra confirmed physical interactions of poly SIS and PPY. The mechanical and electrical testing was done for each concentration of these blends. The incorporation of nano-particles into the poly SIS/PPY blends results in Poly SIS/PPY-V₂O₅ composites. Nano-particles were added in 0-6wt%. The increase in tensile strength with decrease in % strain was observed. The addition of nano-particles to the polymeric blends decrease elongation of poly SIS but increase in strength and stiffness of the films.

Nano-particles because of their size show excellent effects on mechanical properties of composites as composites show good mechanical strength as compare to the polymeric blends.

References:

- [1] T. A. Skotheim, *Handbook of conducting polymers*: CRC press, 1997.
- [2] S. P. Surwade, N. Manohar, and S. K. Manohar, "Origin of bulk nanoscale morphology in conducting polymers," *Macromolecules*, vol. 42, pp. 1792-1795, 2009.
- [3] M. P. Stevens, *Polymer chemistry*: Oxford univ. press New York, 1990.
- [4] L.-X. Wang, X.-G. Li, and Y.-L. Yang, "Preparation, properties and applications of polypyrroles," *Reactive and Functional Polymers*, vol. 47, pp. 125-139, 2001.
- [5] M. Amaike and H. Yamamoto, "Preparation of polypyrrole by emulsion polymerization using hydroxypropyl cellulose," *Polymer journal*, vol. 38, p. 703, 2006.
- [6] R. J. Young and P. A. Lovell, *Introduction to polymers*: CRC press, 2011.
- [7] J. W. P. Lin and L. P. Dudek, "Synthesis and properties of poly (2, 5-thienylene)," *Journal of Polymer Science: Polymer Chemistry Edition*, vol. 18, pp. 2869-2873, 1980.
- [8] S. Bhadra, N. K. Singha, and D. Khastgir, "Electrochemical synthesis of polyaniline and its comparison with chemically synthesized polyaniline," *Journal of applied polymer science*, vol. 104, pp. 1900-1904, 2007.
- [9] K. Kaneto, K. Yoshino, and Y. Inuishi, "Electrical properties of conducting polymer, polythiophene, prepared by electrochemical polymerization," *Japanese Journal of Applied Physics*, vol. 21, p. L567, 1982.
- [10] S. Machida, S. Miyata, and A. Techagumpuch, "Chemical synthesis of highly electrically conductive polypyrrole," *Synthetic metals*, vol. 31, pp. 311-318, 1989.
- [11] H. Letheby, "XXIX.—On the production of a blue substance by the electrolysis of sulphate of aniline," *Journal of the Chemical Society*, vol. 15, pp. 161-163, 1862.
- [12] H. Shirakawa, "Synthesis of polyacetylene," *Handbook of Conducting Polymers*, p. 197, 1997.
- [13] K. M. Molapo, P. M. Ndingili, R. F. Ajayi, G. Mbambisa, S. M. Mailu, N. Njomo, *et al.*, "Electronics of conjugated polymers (I): polyaniline," *International Journal of Electrochemical Science*, vol. 7, pp. 11859-11875, 2012.
- [14] J. L. Bredas and G. B. Street, "Polarons, bipolarons, and solitons in conducting polymers," *Accounts of Chemical Research*, vol. 18, pp. 309-315, 1985.
- [15] A. J. Heeger, S. Kivelson, J. Schrieffer, and W.-P. Su, "Solitons in conducting polymers," *Reviews of Modern Physics*, vol. 60, p. 781, 1988.
- [16] J.-C. Chiang and A. G. MacDiarmid, "'Polyaniline': Protonic acid doping of the emeraldine form to the metallic regime," *Synthetic Metals*, vol. 13, pp. 193-205, 1986.
- [17] T. y. V. Vernitskaya and O. N. Efimov, "Polypyrrole: a conducting polymer; its synthesis, properties and applications," *Russian chemical reviews*, vol. 66, pp. 443-457, 1997.
- [18] R. Ansari, "Polypyrrole conducting electroactive polymers: synthesis and stability studies," *Journal of Chemistry*, vol. 3, pp. 186-201, 2006.
- [19] A. G. MacDiarmid, "Polyaniline and polypyrrole: where are we headed?," *Synthetic Metals*, vol. 84, pp. 27-34, 1997.
- [20] S. Cavallaro, A. Colligiani, and G. Cum, "Oxidative chemical polymerization of pyrrole," *Journal of thermal analysis*, vol. 38, pp. 2649-2655, 1992.
- [21] S. Sadki, P. Schottland, N. Brodie, and G. Sabouraud, "The mechanisms of pyrrole electropolymerization," *Chemical Society Reviews*, vol. 29, pp. 283-293, 2000.
- [22] D. R. Paul, *Polymer blends* vol. 1: Elsevier, 2012.
- [23] M. Xanthos and S. Dagli, "Compatibilization of polymer blends by reactive processing," *Polymer Engineering & Science*, vol. 31, pp. 929-935, 1991.

- [24] L. Utracki, "Economics of polymer blends," *Polymer Engineering & Science*, vol. 22, pp. 1166-1175, 1982.
- [25] D. Paul and S. Newman, "Polymer blends, vol. 2," *Academic, New York*, 1978.
- [26] J. A. Manson, *Polymer blends and composites*: Springer Science & Business Media, 2012.
- [27] I. W. Hamley and I. W. Hamley, *The physics of block copolymers* vol. 19: Oxford University Press Oxford, 1998.
- [28] A. Noshay and J. E. McGrath, *Block copolymers: overview and critical survey*: Elsevier, 2013.
- [29] H. A. Sarvetnick, *Plastisols and organosols*: Van Nostrand Reinhold Co., 1971.
- [30] G. H. Fredrickson and F. S. Bates, "Dynamics of block copolymers: theory and experiment," *Annual Review of Materials Science*, vol. 26, pp. 501-550, 1996.
- [31] S. S. Chin, J. A. Miller, and R. Gobran, "Styrene-isoprene-styrene block copolymer composition and adhesives made therefrom," ed: Google Patents, 1995.
- [32] H. Schmalz, A. Böker, R. Lange, G. Krausch, and V. Abetz, "Synthesis and properties of ABA and ABC triblock copolymers with glassy (A), elastomeric (B), and crystalline (C) blocks," *Macromolecules*, vol. 34, pp. 8720-8729, 2001.
- [33] K. R. Beck, R. Korsmeyer, and R. J. Kunz, "An overview of the glass transition temperature of synthetic polymers," *Journal of Chemical Education*, vol. 61, p. 668, 1984.
- [34] K. Jackson, M. Loadman, C. Jones, and G. Ellis, "Fourier transform Raman spectroscopy of elastomers: An overview," *Spectrochimica Acta Part A: Molecular Spectroscopy*, vol. 46, pp. 217-226, 1990.
- [35] H. Li, X. Zeng, and W. Wu, "Epoxidation of styrene-isoprene-styrene block copolymer and its use for hot-melt pressure sensitive adhesives," *Polymer-Plastics Technology and Engineering*, vol. 47, pp. 978-983, 2008.
- [36] D. Vollath, *Nanomaterials*: Wiley-Vch, 2013.
- [37] C. P. Poole Jr and F. J. Owens, *Introduction to nanotechnology*: John Wiley & Sons, 2003.
- [38] M. A. Ratner and D. Ratner, *Nanotechnology: A gentle introduction to the next big idea*: Prentice Hall Professional, 2003.
- [39] K. N. Thakkar, S. S. Mhatre, and R. Y. Parikh, "Biological synthesis of metallic nanoparticles," *Nanomedicine: Nanotechnology, Biology and Medicine*, vol. 6, pp. 257-262, 2010.
- [40] M. Singh, S. Manikandan, and A. Kumaraguru, "Nanoparticles: A new technology with wide applications," *Research Journal of Nanoscience and Nanotechnology*, vol. 1, pp. 1-11, 2011.
- [41] C. N. R. Rao, A. Müller, and A. K. Cheetham, *The chemistry of nanomaterials: synthesis, properties and applications*: John Wiley & Sons, 2006.
- [42] V. Makarov, A. Love, O. Sinitsyna, S. Makarova, I. Yaminsky, M. Taliansky, *et al.*, "'Green' nanotechnologies: synthesis of metal nanoparticles using plants," *Acta Naturae (англыязычная версия)*, vol. 6, 2014.
- [43] A. K. Mittal, Y. Chisti, and U. C. Banerjee, "Synthesis of metallic nanoparticles using plant extracts," *Biotechnology advances*, vol. 31, pp. 346-356, 2013.
- [44] P. M. Ajayan, L. S. Schadler, and P. V. Braun, *Nanocomposite science and technology*: John Wiley & Sons, 2006.
- [45] B. Fiedler, F. H. Gojny, M. H. Wichmann, M. C. Nolte, and K. Schulte, "Fundamental aspects of nano-reinforced composites," *Composites science and technology*, vol. 66, pp. 3115-3125, 2006.
- [46] X. Li, Y. Yang, and X. Cheng, "Ultrasonic-assisted fabrication of metal matrix nanocomposites," *Journal of Materials Science*, vol. 39, pp. 3211-3212, 2004.
- [47] N. Chawla and Y. L. Shen, "Mechanical behavior of particle reinforced metal matrix composites," *Advanced engineering materials*, vol. 3, pp. 357-370, 2001.
- [48] S. S. Samal and S. Bal, "Carbon nanotube reinforced ceramic matrix composites-a review," 2008.

- [49] M. Sternitzke, "Structural ceramic nanocomposites," *Journal of the European Ceramic Society*, vol. 17, pp. 1061-1082, 1997.
- [50] K. K. Maniar, "Polymeric nanocomposites: A review," *Polymer-Plastics Technology and Engineering*, vol. 43, pp. 427-443, 2004.
- [51] T. Hanemann and D. V. Szabó, "Polymer-nanoparticle composites: from synthesis to modern applications," *Materials*, vol. 3, pp. 3468-3517, 2010.
- [52] J. M. Garces, D. J. Moll, J. Bicerano, R. Fibiger, and D. G. McLeod, "Polymeric nanocomposites for automotive applications," *Advanced Materials*, vol. 12, pp. 1835-1839, 2000.
- [53] P. Kiliaris and C. Papaspyrides, "Polymer/layered silicate (clay) nanocomposites: an overview of flame retardancy," *Progress in Polymer Science*, vol. 35, pp. 902-958, 2010.
- [54] L. A. Utracki, *Clay-containing polymeric nanocomposites* vol. 1: iSmithers Rapra Publishing, 2004.
- [55] C. J. Brabec, A. Cravino, D. Meissner, N. S. Sariciftci, T. Fromherz, M. T. Rispens, *et al.*, "Origin of the open circuit voltage of plastic solar cells," *Advanced Functional Materials*, vol. 11, pp. 374-380, 2001.
- [56] W. S. Khan, N. Hamadneh, and W. A. Khan, "Polymer nanocomposites—synthesis techniques, classification and properties," *Science and applications of Tailored Nanostructures: One Central Press (OCP)*, 2016.
- [57] R. A. Kalgankar, "Polymer nanocomposites based on amorphous copolyester and organo-inorganic nanofillers: a structure and property study," 2007.
- [58] R. Jannapu Reddy, "Preparation, characterization and properties of injection molded graphene nanocomposites," Wichita State University, 2010.
- [59] H. Ishida, S. Campbell, and J. Blackwell, "General approach to nanocomposite preparation," *Chemistry of Materials*, vol. 12, pp. 1260-1267, 2000.
- [60] P. Raveendran, J. Fu, and S. L. Wallen, "Completely "green" synthesis and stabilization of metal nanoparticles," *Journal of the American Chemical Society*, vol. 125, pp. 13940-13941, 2003.
- [61] V. V. T. Padil and M. Černík, "Green synthesis of copper oxide nanoparticles using gum karaya as a biotemplate and their antibacterial application," *International Journal of Nanomedicine*, vol. 8, p. 889, 2013.
- [62] S. Nagarajan and K. A. Kuppusamy, "Extracellular synthesis of zinc oxide nanoparticle using seaweeds of gulf of Mannar, India," *Journal of nanobiotechnology*, vol. 11, p. 39, 2013.
- [63] U. K. Parida, B. K. Bindhani, and P. Nayak, "Green synthesis and characterization of gold nanoparticles using onion (*Allium cepa*) extract," *World Journal of Nano Science and Engineering*, vol. 1, p. 93, 2011.
- [64] N. Ahmad and S. Sharma, "Green synthesis of silver nanoparticles using extracts of *Ananas comosus*," *Green and Sustainable Chemistry*, vol. 2, p. 141, 2012.
- [65] N. Matinise, X. Fuku, K. Kaviyarasu, N. Mayedwa, and M. Maaza, "ZnO nanoparticles via *Moringa oleifera* green synthesis: physical properties & mechanism of formation," *Applied Surface Science*, vol. 406, pp. 339-347, 2017.
- [66] A. Bhattacharya and A. De, "Conducting composites of polypyrrole and polyaniline a review," *Progress in Solid State Chemistry*, vol. 24, pp. 141-181, 1996.
- [67] M. A. De Paoli and W. A. Gazotti, "Conductive polymer blends: preparation, properties and applications," in *Macromolecular Symposia*, 2002, pp. 83-104.
- [68] V. Mano, M. Felisberti, T. Matencio, and M.-A. De Paoli, "Thermal, mechanical and electrochemical behaviour of poly (vinyl chloride)/polypyrrole blends (PVC/PPy)," *Polymer*, vol. 37, pp. 5165-5170, 1996.
- [69] M. Omastová, J. Pionteck, and S. Košina, "Preparation and characterization of electrically conductive polypropylene/polypyrrole composites," *European polymer journal*, vol. 32, pp. 681-689, 1996.

- [70] H. L. Wang and J. E. Fernandez, "Conducting polymer blends: polypyrrole and poly (vinyl methyl ketone)," *Macromolecules*, vol. 25, pp. 6179-6184, 1992.
- [71] S. H. Hosseini and A. A. Entezami, "Conducting polymer blends of polypyrrole with polyvinyl acetate, polystyrene, and polyvinyl chloride based toxic gas sensors," *Journal of applied polymer science*, vol. 90, pp. 49-62, 2003.
- [72] H. L. Wang, L. Toppare, and J. E. Fernandez, "Conducting polymer blends: polythiophene and polypyrrole blends with polystyrene and poly (bisphenol A carbonate)," *Macromolecules*, vol. 23, pp. 1053-1059, 1990.
- [73] Y. Li, S. Wang, Q. Wang, and M. Xing, "A comparison study on mechanical properties of polymer composites reinforced by carbon nanotubes and graphene sheet," *Composites Part B: Engineering*, vol. 133, pp. 35-41, 2018.
- [74] T. Yamamoto and K. Kawaguchi, "Synthesis of composite polymer particles with carbon nanotubes and evaluation of their mechanical properties," *Colloids and Surfaces A: Physicochemical and Engineering Aspects*, vol. 529, pp. 765-770, 2017.
- [75] E. He, S. Wang, Y. Li, and Q. Wang, "Enhanced tribological properties of polymer composites by incorporation of nano-SiO₂ particles: A molecular dynamics simulation study," *Computational Materials Science*, vol. 134, pp. 93-99, 2017.
- [76] Y. Li, S. Wang, and Q. Wang, "Enhancement of tribological properties of polymer composites reinforced by functionalized graphene," *Composites Part B: Engineering*, vol. 120, pp. 83-91, 2017.
- [77] R. K. Nayak, K. K. Mahato, and B. C. Ray, "Water absorption behavior, mechanical and thermal properties of nano TiO₂ enhanced glass fiber reinforced polymer composites," *Composites Part A: Applied Science and Manufacturing*, vol. 90, pp. 736-747, 2016.
- [78] K. K. Mahato, K. Dutta, and B. C. Ray, "Mechanical and thermal behavior of nano-TiO₂ enhanced glass fibre reinforced polymeric composites at various crosshead speeds," 2018.
- [79] P. Rajeshwari and T. Dey, "Novel HDPE nanocomposites containing aluminum nitride (nano) particles: Micro-structural and nano-mechanical properties correlation," *Materials Chemistry and Physics*, vol. 190, pp. 175-186, 2017.
- [80] P. M. Rahman, V. A. Mujeeb, K. Muraleedharan, and S. K. Thomas, "Chitosan/nano ZnO composite films: enhanced mechanical, antimicrobial and dielectric properties," *Arabian Journal of Chemistry*, 2016.
- [81] M. Mohammadi, F. Ziaie, A. Majdabadi, A. Akhavan, and M. Shafaei, "Improvement of mechanical and thermal properties of high energy electron beam irradiated HDPE/hydroxyapatite nano-composite," *Radiation Physics and Chemistry*, vol. 130, pp. 229-235, 2017.
- [82] J. Sha, Z. Lv, J. Li, Z. Zhang, and J. Dai, "Effect of in-situ grown SiC nanowires on mechanical properties of short carbon fiber-reinforced polymer composites," *Materials Letters*, vol. 199, pp. 17-20, 2017.
- [83] S. Mondal and D. Khastgir, "Elastomer reinforcement by graphene nanoplatelets and synergistic improvements of electrical and mechanical properties of composites by hybrid nano fillers of graphene-carbon black & graphene-MWCNT," *Composites Part A: Applied Science and Manufacturing*, vol. 102, pp. 154-165, 2017.
- [84] M. K. Pitchan, S. Bhowmik, M. Balachandran, and M. Abraham, "Effect of surface functionalization on mechanical properties and decomposition kinetics of high performance polyetherimide/MWCNT nano composites," *Composites Part A: Applied Science and Manufacturing*, vol. 90, pp. 147-160, 2016.

- [85] A. Alam, Y. Zhang, H.-C. Kuan, S.-H. Lee, and J. Ma, "Polymer composite hydrogels containing carbon nanomaterials—Morphology and mechanical and functional performance," *Progress in Polymer Science*, vol. 77, pp. 1-18, 2018.
- [86] H. Assaedi, F. Shaikh, and I. M. Low, "Effect of nano-clay on mechanical and thermal properties of geopolymer," *Journal of Asian Ceramic Societies*, vol. 4, pp. 19-28, 2016.
- [87] Y. Li, S. Wang, and Q. Wang, "A molecular dynamics simulation study on enhancement of mechanical and tribological properties of polymer composites by introduction of graphene," *Carbon*, vol. 111, pp. 538-545, 2017.
- [88] S. Iravani, "Green synthesis of metal nanoparticles using plants," *Green Chemistry*, vol. 13, pp. 2638-2650, 2011.
- [89] H. N. Graham, "Green tea composition, consumption, and polyphenol chemistry," *Preventive medicine*, vol. 21, pp. 334-350, 1992.
- [90] D. Robin, "Implementation, Analytical Characterization and Application of a Novel Portable XRF/XRD Instrument," 2012.
- [91] L. Whittig and W. Allardice, "X-ray diffraction techniques," *Methods of soil analysis. Part 1. Physical and mineralogical methods*, pp. 331-362, 1986.
- [92] H. P. Klug and L. E. Alexander, "X-ray diffraction procedures: for polycrystalline and amorphous materials," *X-Ray Diffraction Procedures: For Polycrystalline and Amorphous Materials, 2nd Edition*, by Harold P. Klug, Leroy E. Alexander, pp. 992. ISBN 0-471-49369-4. Wiley-VCH, May 1974., p. 992, 1974.
- [93] R. Jenkins and R. L. Snyder, *Introduction to X-ray Powder Diffractometry (Volume 138)*: Wiley Online Library, 1996.
- [94] B. D. Cullity and S. R. Stock, *Elements of X-ray Diffraction*: Pearson Education, 2014.
- [95] O. Faix, "Fourier transform infrared spectroscopy," in *Methods in lignin chemistry*, ed: Springer, 1992, pp. 83-109.
- [96] J. Bates, "Fourier transform infrared spectroscopy," *Science*, vol. 191, pp. 31-37, 1976.
- [97] B. C. Smith, *Fundamentals of Fourier transform infrared spectroscopy*: CRC press, 2011.
- [98] D. DeGaetano, J. A. Siegel, and K. Klomprens, "A comparison of three techniques developed for sampling and analysis of gunshot residue by scanning electron microscopy/energy-dispersive X-ray analysis (SEM-EDX)," *Journal of Forensic Science*, vol. 37, pp. 281-300, 1992.
- [99] H. Todokoro and T. Otaka, "Scanning electron microscope," ed: Google Patents, 1995.
- [100] N. J. Unakar, J. Y. Tsui, and C. V. Harding, "Scanning electron microscopy," *Ophthalmic Research*, vol. 13, pp. 20-35, 1981.
- [101] L. Reimer, *Scanning electron microscopy: physics of image formation and microanalysis* vol. 45: Springer, 2013.
- [102] J. Goldstein, *Practical scanning electron microscopy: electron and ion microprobe analysis*: Springer Science & Business Media, 2012.
- [103] J. I. Goldstein, D. E. Newbury, J. R. Michael, N. W. Ritchie, J. H. J. Scott, and D. C. Joy, *Scanning electron microscopy and X-ray microanalysis*: Springer, 2017.
- [104] R. F. Landel and L. E. Nielsen, *Mechanical properties of polymers and composites*: CRC press, 1993.
- [105] E. Part, E. Part, G. Part, and A. Annex, "Form and Style for ASTM Standards," ed: ASTM, Philadelphia, 1989.
- [106] J. R. Davis, *Tensile testing*: ASM international, 2004.
- [107] Y. Li, J.-L. Kuang, Y. Lu, and W.-B. Cao, "Facile Synthesis, Characterization of Flower-Like Vanadium Pentoxide Powders and Their Photocatalytic Behavior," *Acta Metallurgica Sinica (English letters)*, vol. 30, pp. 1017-1026, 2017.

- [108] A. T. Raj, K. Ramanujan, S. Thangavel, S. Gopalakrishnan, N. Raghavan, and G. Venugopal, "Facile synthesis of vanadium-pentoxide nanoparticles and study on their electrochemical, photocatalytic properties," *Journal of nanoscience and nanotechnology*, vol. 15, pp. 3802-3808, 2015.
- [109] S. Senthilkumar and T. Sivakumar, "Green tea (*Camellia sinensis*) mediated synthesis of zinc oxide (ZnO) nanoparticles and studies on their antimicrobial activities," *Int J Pharm Pharm Sci*, vol. 6, pp. 461-465, 2014.
- [110] M. A. Chougule, S. G. Pawar, P. R. Godse, R. N. Mulik, S. Sen, and V. B. Patil, "Synthesis and characterization of polypyrrole (PPy) thin films," *Soft Nanoscience Letters*, vol. 1, p. 6, 2011.
- [111] M. Sharma, G. I. Waterhouse, S. W. Loader, S. Garg, and D. Svirskis, "High surface area polypyrrole scaffolds for tunable drug delivery," *International journal of pharmaceuticals*, vol. 443, pp. 163-168, 2013.